1 **Comparison of key absorption and optical properties between pure**

2 **and transported anthropogenic dust over East and Central Asia**

3 Jianrong Bi[1], Jianping Huang[1*], Brent Holben[2], Guolong Zhang[1]

5 [1]Key Laboratory for Semi-Arid Climate Change of the Ministry of Education, College of

6 Atmospheric Sciences, Lanzhou University, Lanzhou, 730000, China

7 [2]NASA Goddard Space Flight Center, Greenbelt, Maryland, USA

9 *Submitted to: ACP Special Issue*

27 --

28 *Correspondence to:* Jianping Huang (hjp@lzu.edu.cn)

Abstract. Asian dust particulate is one of the primary aerosol constituents in the Earth-atmosphere system that exerts profound influences on environmental quality, human health, marine biogeochemical cycle and Earth's climate. To date, the absorptive capacity of dust aerosol generated from Asian desert region is still an open question. In this article, we compile columnar key absorption and optical properties of mineral dust over East and Central Asia areas by utilizing the multi-year quality assured datasets observed at 13 sites of the Aerosol Robotic Network (AERONET). We identify two types of Asian dust according to threshold criteria from previously published literature. (I) The particles with high aerosol optical depth at 440 nm ($AOD_{440} \geq 0.4$) and low Ångström wavelength exponent at 440-870 nm ($\alpha < 0.2$) are defined as Pure Dust (PDU) that decrease disturbance of other non-dust aerosols and keep high accuracy of pure Asian dust. (II) The particles with $AOD_{440} \geq 0.4$ and $0.2 < \alpha < 0.6$ are designated as Transported Anthropogenic Dust (TDU), which are mainly dominated by dust aerosol and might mix with other anthropogenic aerosol types. Our results reveal that the primary components of high AOD days are predominant by dust over East and Central Asia regions even if their variations rely on different sources, distance from the source, emission mechanisms, and meteorological characteristics. The overall mean and standard deviation of single-scattering albedo, asymmetry factor, real part and imaginary part of complex refractive index at 550 nm for Asian PDU are 0.935±0.014, 0.742±0.008, 1.526±0.029, 0.00226±0.00056, respectively, while corresponding values are 0.921±0.021, 0.723±0.009, 1.521±0.025, and 0.00364±0.0014 for Asian TDU. Aerosol shortwave direct radiative effects at the top of the atmosphere (TOA), at the surface (SFC), and in the atmospheric layer (ATM) for Asian PDU ($\alpha < 0.2$) and TDU ($0.2 < \alpha < 0.6$) computed in this study, are a factor of 2 smaller than the results of Optical Properties of Aerosols and Clouds (OPAC) Mineral accumulated (Mineral acc.) and transported (Mineral tran.) modes. Therefore, we are convinced that our results hold promise of updating and improving accuracies of Asian dust characteristics in present-day remote sensing applications and regional or global

climate models.

1. Introduction

Airborne dust particle (also called mineral dust) is recognized as one of the most important aerosol species in the tropospheric atmosphere, which accounts for about 30% of the total aerosol loading and extinction aerosol optical depth on a global scale (Perlwitz et al., 2001; Kinne et al., 2006; Chin et al., 2009; Huang et al., 2014). High concentrations of dust aerosols hanging over desert source regions and invasive downstream areas would seriously exacerbate air quality, degrade visibility, affect transportation safety, and do adverse effects on public health during the prevalent seasons of dust storms (Chan et al., 2008; Morman and Plumlee, 2013; Wang et al., 2016). When mineral dusts are deposited onto the Earth's surface, they play a key role in biogeochemical cycles of terrestrial ecosystem or ocean (Okin et al., 2004; Jickells et al., 2005; Shao et al., 2011), as well as alter snow and ice albedo (Aoki et al., 2006; Huang et al., 2011; Wang et al., 2014). Last but not least, dust particles can modulate the Earth's energy budget and drive the climate change directly by scattering and absorption of solar/terrestrial radiation (Charlson et al., 1992; Wang et al., 2010b; Huang et al., 2014), and indirectly by acting as effective cloud condensation nuclei or ice nuclei, influencing the cloud microphysics and precipitation processes (Ramanathan et al., 2001; Rosenfeld et al., 2001; DeMott et al., 2003; Huang et al., 2005, 2006, 2010a; Wang et al., 2010c; Creamean et al., 2013). Numerous studies (Sokolik and Toon, 1999; Lafon et al., 2004, 2006) have confirmed that dust particle is one kind of light absorbing substances, and its mass absorption efficiencies at 325 nm (0.06~0.12 m^2/g) are about 6 times larger than that at 660 nm (0.01~0.02 m^2/g), owing to the greater absorbing potential of iron oxides at short wavelengths (Alfaro et al., 2004). However, the way of iron oxides mixed with quartz or clay is complicated and strongly impacts the resulting absorption (Claquin et al., 1998, 1999; Sokolik and Toon, 1999). And these mineralogical studies indicate that a lack of consideration of these mixing mechanisms is a significant limitation of the previous dust absorption computations. Although the absorptive ability of dust is two orders of magnitude

88 lower than for black carbon (Yang et al., 2009), the atmospheric mass loading of the

89 former is the same magnitude larger than that of the latter, leading to the total

90 absorption in solar spectrum comparable to black carbon. Chin et al. (2009) evaluated

91 that dust may account for about 53% of global averaged aerosol absorption optical

92 depth at 550 nm, which undoubtedly changes the aforementioned

93 dust-cloud-precipitation interaction and exerts a significant effect on hydrological

94 cycle of the Earth-atmosphere system.

95 East and Central Asia territories are the major source regions of dust aerosols on

96 Earth, which produce a large amount of dust particles every year that become

97 entrained into the upper atmosphere by cold fronts (Zhang et al., 1997; Huang et al.,

98 2009, 2010a, 2014). They can travel over thousands of kilometers, even across the

99 Pacific Ocean and reach the western coast of North America about one week with the

100 prevailing westerly wind (Husar et al., 2001; Uno et al., 2009, 2011), and then modify

101 the climate and environment over extensive area of Asia-Pacific rim. Thus far, there

102 have been a great deal of fruitful field campaigns for exploring Asian dust (e.g.,

103 U.S.S.R.-U.S., ACE-Asia, ADEC, PACDEX, EAST-AIRC), however, most focus on

104 intensive observation period (Golitsyn and Gillette, 1993; Huebert et al., 2003;

105 Nakajima et al., 2003; Mikami et al., 2006; Huang et al., 2008a; Li et al., 2011) and

106 lack of long-term and quantitative knowledge of dust optical, microphysical

107 characteristics (especially absorption properties) and chemical compositions over

108 these regions. Hence, the absorptive capacity of Asian dust aerosol is still an

109 outstanding issue. The variations of dust optical features in model calculations are

110 closely related to the uncertainties in particle size distribution and prescribing a value

111 for complex refractive index. Whereas the key parameters of Asian dust aerosols in

112 present-day climate models are still prescribed to the predetermined properties of

113 Saharan mineral dust.

114 Wang et al. (2004) inferred the refractive index of pure minerals at Qira in

115 Taklimakan Desert during April 12-14, 2002 via combination of theoretical

116 calculation and composition analysis of aerosol samples, and showed that the value of

117 imaginary part is 0.00411 at 500 nm, which is consistent with the Central Asian dust

of 0.004±0.001 (Tadzhikistan Desert; Sokolik and Golitsyn, 1993). Uchiyama et al. (2005) determined the single-scattering albedo (SSA) of Aeolian dust from sky radiometer and in situ measurements, and concluded that unpolluted Aeolian dust (source from Taklimakan Desert) has low absorption (with SSA_{500} of 0.93~0.97). Kim et al. (2004) analyzed multiyear sky radiation measurements over East Asian sites of Skyradiometer Network (Nakajima et al., 1996; Takamura et al., 2004) and showed the SSA_{500} of dust particles are around 0.9 in arid Dunhuang of northwest China and Mandalgovi Gobi desert in Mongolia. Bi et al. (2014) also reported the similar SSA_{550} (0.91~0.97) of dust aerosol at Dunhuang during spring of 2012. Xu et al. (2004) gained SSA_{530} of 0.95±0.05 in Yulin, China, from a Radiance Research nephelometer and a Particle Soot Absorption Photometer (PSAP) and suggested that both desert dust and local pollution sources contributed to the aerosol loading in Yulin during April 2001. Whereas Ge et al. (2010) examined dust aerosol optical properties at Zhangye (a semiarid area of northwest China) from multifilter rotating shadowband radiometer (MFRSR) during spring of 2008 and found that although there are low aerosol optical depth values (AOD_{670} ranging from 0.07~0.25), dust particles have strong absorption (with SSA_{500} of 0.75±0.02) due to mixing with local anthropogenic pollutants. This result is close to the New Delhi over India (0.74~0.84 for SSA_{500}; Pandithurai et al., 2008). Lafon et al. (2006) revealed that due to containing of less calcite and higher fraction of iron oxide-clay aggregates, mineral dusts in Niger (Banizoumbou, 13°31′N, 2°38′E) have much lower SSA in the visible wavelengths than that of Chinese (Ulan Buh, 39°26′N, 105°40′E) and Tunisian (Maouna, 33°01′N, 10°40′E) desert locations. Therefore, complete clarification of the climate-relevant impacts of Asian dust aerosols requires extensive and long-term measurements of the optical, microphysical and chemical properties, along with their spatial and temporal distributions.

There have been several world-famous aerosol long-term monitoring networks over Asian region for examining aerosol features and its radiative effects, for instance, AERONET—AErosol RObotic NETwork (Holben et al., 1998), SKYNET—aerosol-cloud-radiation interaction ground-based observation network (Nakajima et al., 1996; Takamura et al., 2004; Che et al., 2008), and

CARSNET—China Aerosol Remote Sensing Network (Che et al., 2009a, 2014, 2015). In this paper, we investigate optical characteristics of Asian dust from multi-year AERONET measurements at 13 sites in and around arid or semi-arid regions of East and Central Asian desert sources. The key quantities include single-scattering albedo (SSA), asymmetry factor (ASY), real part (Re) and imaginary part (Ri) of complex refractive index, volume size distribution (dV/dlnr), which are needed for climate simulating and remote sensing applications. We mainly compare the vital absorption and optical properties between pure and transported anthropogenic dust over East and Central Asia. This article is arranged as follows. Section 2 introduces the site description and measurement. The identification method and detailed Asian dust optical features are described in Section 3. Discussion of spectral absorption behaviors of different dust aerosol types are given in Section 4 and followed by the Summary in Section 5.

2. Site Description and Measurement

2.1. Site Description

In this article, we select 13 AERONET sites located in arid or semi-arid Asian regions (see Fig. 1), which are recognized as the primarily active centre of dust storms. These drylands are very sensitive to climate change and human activities and would accelerate drought expansion by the end of twenty-first century (Zheng et al., 2009; Huang et al., 2016). Eight sites over East Asian region are labeled with red colors, and five sites over Central Asian area are labeled with blue colors. The major Great deserts or Gobi deserts along with plateaus are marked with black font (e.g., Great Gobi desert in Mongolia, Taklimakan Desert, Thar Desert, Karakum Desert, Tibetan Plateau, Loess Plateau, and Iranian Plateau). In order to quantitatively explore detailed spectral absorptive characteristics of dust aerosols over East and Central Asia, we choose four East Asian sites (SACOL, Dalanzadgad, Beijing, and Yulin) and four Central Asian sites (Dushanbe, Karachi, Kandahar, and IASBS). They consist of: SACOL located over Loess Plateau of northwest China (Huang et al., 2008b; Guan et al., 2009; Huang et al., 2010b; Wang et al., 2010a), Dalanzadgad in the Great Gobi of

177 southern Mongolia (Eck et al., 2005), Beijing in the downwind of Inner Mongolia

178 (Xia et al., 2007), Yulin on the southwestern fringe of the Mu Us desert in northwest

179 China (Xu et al., 2004; Che et al., 2009b, 2015), Dushanbe in Tadzhikistan situated at

180 the transport corridor of Central Asian desert dust (i.e. Karakum Desert; Golitsyn and

181 Gillette, 1993), Karachi located in the southern margin of Thar Desert in Pakistan and

182 about 20 km from the east coast of Arabian Sea (Alam et al., 2011), Kandahar in the

183 arid area of southern Afghanistan, IASBS on the Iranian Plateau of northwest Iran.

184 **2.2. Sun Photometer Measurements**

185 AERONET is an internationally federated global ground-based aerosol monitoring

186 network utilizing Cimel sun photometer, which comprises more than 500 sites all over

187 the world (Holben et al., 1998). The Cimel Electronique sun photometer (CE-318)

188 takes measurements of sun direct irradiances at multiple discrete channels within the

189 spectral range of 340-1640 nm, which can be calculated aerosol optical depth (AOD)

190 and columnar water vapor content (WVC) in centimeter. Furthermore, the instrument

191 can perform angular distribution of sky radiances at 440, 675, 870, and 1020 nm

192 (nominal wavelengths), which can be simultaneously retrieved aerosol volume size

193 distribution, complex refractive index, single-scattering albedo, and asymmetry factor

194 under cloudless condition (Dubovik and King, 2000; Dubovik et al., 2002a, 2006).

195 The total accuracy in AOD for a newly calibrated field instrument is about

196 0.010-0.021 (Eck et al., 1999). The retrieval errors of SSA, ASY, Ri, and Re are

197 anticipated to be 0.03-0.05, 0.04, 30%-50%, and 0.025-0.04, respectively, relying on

198 aerosol types and loading (Dubovik et al., 2000). It should be borne in mind that these

199 uncertainties are valid for AOD_{440} ≥0.4 and for solar zenith angle >50° (Level 2.0

200 product), and the retrieval errors will become much greater when AOD_{440} <0.4. The

201 datasets of selected 13 AERONET sites in this study come from the Level2.0 product,

202 which are pre- and post-field calibrated, automatically cloud screened, and

203 quality-assured (Smirnov et al., 2000). In addition, a mixture of randomly oriented

204 polydisperse spheroid particle shape assumption with a fixed aspect ratio distribution

205 is applied to retrieve key optical properties of Asian dust (Dubovik, et al., 2002a,

206 2006). Fu et al. (2009) have concluded that Mie-based single-scattering properties of

207 spheroidal dust aerosols are well suited in radiative flux calculations.

3. Asian Dust Optical Properties

209 A great amount of publications have verified that mineral dust aerosols are
210 commonly predominant by large particles with coarse mode (radii>0.6 μm), which are
211 the essential feature differentiating the dust from fine-mode dominated biomass
212 burning and urban-industrial aerosols (Dubovik et al., 2002b; Eck et al., 2005; Bi et
213 al., 2011, 2014; Kim et al., 2011; Che et al., 2013). In other word, the values of
214 Ångström exponent at 440-870 nm (α) for dust aerosols usually range between -0.1 to
215 0.6. As pointed out by Smirnov et al. (2002) and Dubovik et al. (2002b), sea salt
216 aerosol is also dominant by coarse mode and has small Ångström exponent (~0.3-0.7)
217 but with low AOD_{440} (~0.15-0.2) compared with dust aerosol. Moreover, the selected
218 desert locations in this study are mostly not affected by sea salt. By virtue of these
219 differences, we can distinguish Asian dust aerosols from other fine-mode dominated
220 non-dust particles. The criteria of two thresholds are put forward. (I) The particles
221 with high aerosol optical depth at 440 nm ($AOD_{440} \geq 0.4$) and low Ångström
222 wavelength exponent at 440-870 nm ($\alpha < 0.2$) are defined as Pure Dust (PDU) that
223 keep high accuracy of pure Asian dust and eliminate most fine mode aerosols. (II) The
224 particles with $AOD_{440} \geq 0.4$ and $0.2 < \alpha < 0.6$ are designated as Transported
225 Anthropogenic Dust (TDU), which are mainly dominated by dust and might mix with
226 other anthropogenic aerosol types during transportation. The definition of
227 anthropogenic dust in this study is different from earlier literature (Tegen and Fung,
228 1995; Prospero et al., 2002; Huang et al., 2015), which define that anthropogenic dust
229 is primarily produced by various human activities on disturbed soils (e.g., agricultural
230 practices, industrial activity, transportation, desertification and deforestation). It is still
231 a huge challenge to discriminate between natural and anthropogenic components of
232 dust aerosols by using current technology, AERONET products or in-situ
233 measurements. Recently, Ginoux et al. (2012) first estimated that anthropogenic
234 sources globally account for 25% based on Moderate Resolution Imaging
235 Spectroradiometer (MODIS) Deep Blue dust optical depth in conjunction with other

land use data sets. Huang et al. (2015) proposed a new algorithm for distinguishing anthropogenic dust from natural dust by using Cloud-Aerosol Lidar and Infrared Pathfinder Satellite Observation (CALIPSO) and planetary boundary layer (PBL) height retrievals along with MODIS land cover data set. They revealed that anthropogenic dust produced by human activities mainly comes from semi-arid and semi-humid regions and is generally mixed with other types of aerosols within the PBL that is more spherical than natural dust. Thereby, we assume that anthropogenic dust aerosol originated from Asian arid or semi-arid areas has got smaller size distribution (thus larger Ångström exponent) than that of pure natural dust.

Before insight into dust aerosol optical characteristics, we first analyze the occurrence frequency of Asian dust over the study region that significantly affects the intensity and distribution of mineral dust loading. Figure 2 depicts the total number days of each month for Pure Dust ($\alpha<0.2$) and transported Anthropogenic Dust ($0.2<\alpha<0.6$) at selected four East Asian sites and four Central Asian sites. The dust events at four East Asian sites primarily concentrate on springtime and corresponding peak days for PDU and TDU both appear in April. This is greatly attributed to the intrusion of dust particles during spring when dust storms are prevalent over these regions (Wang et al., 2008). For SACOL and Beijing sites, both the PDU and TDU days also occur in whole year except for autumn when is the rainy season, which is linked with long-range transport of dust particulates from desert source areas and locally anthropogenic dust (e.g., agricultural cultivation, overgrazing, desertification, industrial and constructed dust in urbanization). Shen et al. (2016) have demonstrated that urban fugitive dust generated by road transport and urban construction contributes to more than 70% of particulate matter ($PM_{2.5}$) in northern China. The dust episodes in Dushanbe of Tadzhikistan mostly happen from July to October, which are the peak seasons of dust storms (Golitsyn and Gillette, 1993). For Karachi site in Pakistan, the dust activities take place in spring and summer seasons. This is because the region is not affected by the summer monsoon, leaving the land surface sufficiently dry, and hence susceptible to wind erosion by strong winds and meso-scale thunderstorm events typical of this time of year (Alizadeh Choobari et al.,

266 2014). In addition, the transport of summer dust plumes from the Arabian Peninsula

267 can partially contribute dust particles to Karachi site. Note that the occurred months of

268 PDU cases are nearly different from TDU cases at Dalanzadgad, Kandahar, and

269 IASBS sites, suggesting that dust aerosols over these areas are rarely affected by

270 anthropogenic pollutants. For Kandahar site in Afghanistan, the limited sampling days

271 to some extent may affect the statistical results. Generally, the aforementioned

272 occurrence frequency of dust storms over diverse sites are principally dependent on

273 different climatic regime and synoptic pattern, for instance, geographical location,

274 atmospheric circulation, wet season and dry season.

275   Table 1 summarizes the site information, sampling period, overall average optical

276 properties at 550 nm (e.g., SSA, ASY, Re, Ri, and Ångström exponent at 440-870 nm)

277 for Asian PDU ($\alpha<0.2$), and total number of PDU and TDU ($0.2<\alpha<0.6$) days. Note

278 that dust optical feature at a common 550 nm wavelength is utilized here, which can

279 be derived from logarithmic interpolation between 440 and 675 nm. It is worth

280 pointing out that the absorption and optical properties of dust aerosols at two

281 Dunhuang sites exhibit consistent features despite of different sampling periods,

282 which indicate that the chemical composition of dust aerosol at Dunhuang area

283 remains relatively stable.

284   The SSA or Ri of complex refractive index can characterize the absorptive

285 capability of dust aerosols, and determine the sign (cooling or heating, depending on

286 the planetary albedo) of the radiative forcing (Hansen et al., 1997). Both two

287 quantities are mainly relied on the ferric oxide content in mineral dust (Sokolik and

288 Toon, 1999). Figure 3 illustrates the overall average spectral behavior of key optical

289 properties for PDU ($\alpha<0.2$) and TDU ($0.2<\alpha<0.6$) at selected four East Asian sites.

290 The SSA, ASY, Re and Ri of complex refractive index as a function of wavelength

291 (440, 675, 870, and 1020 nm) are presented. For all cases, the spectral behaviors of

292 aerosol optical parameters exhibit similar features, which can be representative of

293 typical patterns of Asian dust. The SSA values systematically increase with

294 wavelength at 440-675 nm and keep almost neutral or slight increase for the

295 wavelengths greater than 675 nm, which is consistent with the previous results of dust

aerosols (Dubovik et al., 2002b; Eck et al., 2005; Bi et al., 2011). In contrast, an opposite pattern is displayed by imaginary part of refractive index, namely, Ri values dramatically decrease from 440 nm to 675 nm, and preserve invariant from 675 nm to 1020 nm. These variations indicate that Asian dust aerosols have got much stronger absorptive ability at shorter wavelength. Alfaro et al. (2004) implied that the absorption capacity of soil dust increase linearly with iron oxide content, and estimated SSA at 325 nm (~0.80) is much lower than that at 660 nm (~0.95). Sokolik and Toon (1999) revealed that ferric iron oxides (e.g., hematite and goethite) are often internally mixed with clay minerals and result in significant dust absorption in the UV/visible wavelengths. Hence, the spectral variations of SSA and Ri with wavelengths are attributable to the domination of coarse-mode dust particles that have larger light absorption in the blue spectral band as mentioned above. It is worth noting that spectral ASY values remarkably reduce from 440 nm to 675 nm, and are almost constant at 675-1020 nm range. This suggests that Asian dust aerosols have much stronger scattering at 440 nm than other longer visible wavebands, due to the contribution of coarse mode particles. By contrast, the spectral behavior of Re is not obvious for PDU and TDU at all sites, and the mean Re values at 440 nm vary between 1.50 and 1.56. Although there are 18 years continuous AERONET datasets at Dalanzadgad site, the effective days of PDU and TDU are only 8 and 6 days, respectively, almost appearing in springtime period. There are no identifiable differences for dust absorption properties between PDU and TDU cases for Dalanzadgad, which indicates again that the site is hardly influenced by anthropogenic pollutants. The spectral discrepancies of optical characteristics between PDU and TDU at other three sites show much more apparent than Dalanzadgad, which is ascribed to these regions are not only affected by dust aerosols, but also including local anthropogenic emissions, for instance, urban-industry, coal fuel combustion, biomass burning, mobile source emissions, and agricultural dust (Xu et al., 2004; Xia et al., 2007; Che et al., 2015; Bi et al., 2011; Wang et al., 2015).

Figure 4 is the same as Figure 3, but for selected four Central Asian sites. The wavelength dependencies of PDU and TDU cases at Central Asian sites are consonant

326   with that of East Asian sites, despite of somewhat different variations of magnitude

327   and amplitude. This is expected, because the East Asian desert sites are very close to

328   the Central Asian desert locations and remain similar chemical compositions of dust

329   aerosols (Wang et al., 2004). The spectral behaviors of dust optical properties for

330   PDU at Kandahar and IASBS sites are nearly the same as TDU cases, which agrees

331   well with the consistent variability of occurrence of dust storms. The wavelength

332   dependency of dust characteristics for PDU at Dushanbe and Karachi presents large

333   differences with TDU case, which is also likely due to the influence of local

334   anthropogenic pollutions. Furthermore, the standard deviation of PDU is far less than

335   that of TDU at all wavelengths, suggesting that the robustness of PDU recognition

336   method.

337   Particle size distribution is another critical agent for deciding the optical and

338   radiative properties of dust aerosol. Nakajima et al. (1996) and Dubovik and King

339   (2000) uncovered that based on the spherical Mie theory, the retrieval errors of

340   volume size distribution do not exceed 10% for intermediate particle size ($0.1 \leq r \leq 7$

341   μm) and may greatly increase to 35-100% at the edges of size range ($r < 0.1$ μm or $r > 7$

342   μm). As mentioned above, a polydisperse, randomly oriented spheroid method is

343   utilized in this study, which is demonstrated to remove the artificially increased size

344   distribution of fine particle mode with $AOD_{440} \geq 0.4$ and for solar zenith angle $> 50°$.

345   Additionally, the large errors at the edges do not significantly affect the derivation of

346   the main features of the particle size distribution (concentration, median and effective

347   radii, etc.), because typical dust aerosol size distributions have low values at the edges

348   of retrieval size interval (Dubovik et al., 2002a). Figure 5 delineates the overall

349   average columnar aerosol volume size distributions (dV/dlnr, 0.05 μm$\leq r \leq$15 μm) for

350   Pure Dust ($\alpha < 0.2$) and Transported Anthropogenic Dust ($0.2 < \alpha < 0.6$) at selected 13

351   AERONET sites. Corresponding AOD_{440} and effective radius of coarse mode (r_{coarse})

352   in μm are also shown. It is apparent that the dV/dlnr exhibits a typical bimodal

353   structure and is dominant by coarse mode for PDU and TDU at all sites. The dV/dlnr

354   peak of coarse mode particle varies dramatically and appears at a radius $r_{Vc} \sim 2.24$ μm

355   for all PDU cases and $r_{Vc} \sim 2.0$-3.0 μm for TDU cases, while the corresponding peak of

fine mode particle arises at a radius r_{Vf} ~0.09-0.12 μm. The dV/dlnr peak and effective radius (r_{coarse}) of coarse mode particles strikingly increase with the increase of AOD ascribed to the intrusion of dust particles. For instance, the AOD_{440}, dV/dlnr peak values of coarse mode, and r_{coarse} for PDU at Minqin site are 0.48, 0.31 $μm^3/μm^2$, and 1.74 μm, respectively, and corresponding values are 1.13, 0.77 $μm^3/μm^2$, and 1.93 μm at Lahore site, as shown in Fig. 5(a). The average volume median radii of fine-mode and coarse-mode particles for PDU are 0.159 μm and 2.157 μm, respectively, and 0.140 μm and 2.267 μm for TDU (see Table. 2). The mean volume concentration ratio of coarse mode to fine mode particles (C_{vc}/C_{vf}) for Pure Dust is about 18 (varying between 11~31) over East and Central Asia, which is close to the average of ~20 at Dunhuang_LZU during the spring of 2012 (Bi et al., 2014), and much less than that over Saharan pure desert domain (~50) (Dubovik et al., 2002b). The dV/dlnr peak of coarse mode for TDU is clearly smaller than that for PDU, and corresponding mean C_{vc}/C_{vf} value is 9 (~5-11). We attribute the high fractions of coarse-mode particles to high AOD and low Ångström exponent values.

In this paper, we postulate that Asian dust particles only possess scattering and absorption characteristics. And the absorption AOD value (AAOD) at a specific wavelength can be obtained from SSA and AOD, namely, $AAOD_\lambda=(1-SSA_\lambda)\times AOD_\lambda$, where λ is the wavelength. Thereby, the corresponding absorption Ångström exponent at 440-870 nm (AAE) is calculated from spectral AAOD values by using a log-linear fitting algorithm. Figure 6 outlines the total average Ångström exponent (α) and absorption Ångström exponent at 440-870 nm, volume concentration of coarse mode in $μm^3/μm^2$, and volume median radius of coarse mode in μm for TDU ($0.2<\alpha<0.6$) and PDU ($\alpha<0.2$) at selected AERONET sites. There are very big differences of all quantities between PDU and TDU cases, except for some sites (e.g., Dunhuang and Minqin). The primary reason is that we only acquire limited datasets of dust days during spring time at Dunhuang and Minqin sites, which are hardly affected by other anthropogenic pollutants. The AE values of TDU show remarkable changes among each site, ranging from 0.24 to 0.44, whereas corresponding values of PDU keep comparatively slight variations for selected 13 sites (~0.04-0.15). Furthermore, all the

386   AAE values of PDU are greater than 1.5, ranging between 1.65 and 2.36, and the

387   AAE of TDU vary from 1.2 to 2.3. We can conclude that the Asian pure dust aerosols

388   have got AE values smaller than 0.2 and corresponding AAE larger than 1.50, which

389   is another typical feature distinguishing with other non-dust aerosols. Yang et al.

390   (2009) attributed the high AAE values of dust aerosol in China to the presence of

391   ferric oxides. It is evident that volume concentrations of coarse mode for PDU are

392   significantly higher than TDU case, which is expected for the more coarse-mode

393   particles in PDU. While the volume median radius of coarse mode for TDU is greater

394   than PDU case, although there are some smaller values for TDU at Dalanzadgad and

395   Yulin sites. This is owing to dust particles at these sites usually mix with other

396   anthropogenic aerosol species and substantially enhance their median radii.

397   Figure 7 characterizes the overall mean optical properties (e.g., SSA, ASY, Re,

398   and Ri) at 440 nm for selected 13 sites. In general, the absorption capacity of PDU is

399   less than that for TDU. That is, higher SSA and smaller Ri values for PDU, except for

400   Dalanzadgad site. A reasonable interpretation is that threshold criterion method for

401   PDU in this study has effectively eliminated the fine mode aerosols, which are mostly

402   the much stronger absorbing aerosols (e.g., soot and biomass burning aerosol) over

403   East and Central Asia but weaker absorbing pollution aerosols (i.e., sulfate and nitrate)

404   over Dalanzadgad. Wu et al. (2012, 2014) have documented that sulfate and nitrate in

405   background atmosphere most likely originated directly from surface soil at the north

406   and south edges of Taklimakan desert and comprised steadily about 4% of dust

407   particulate matters, which could partially explain our results. Additionally, the overall

408   mean ASY and Re of PDU are greater than that of TDU, which again verifies that the

409   Asian pure dust has got much stronger forward scattering ability than the mixture of

410   Asian dust. Note that the standard deviation of SSA and Ri for PDU is a factor of two

411   to four lower than those from TDU. And the total average values of SSA, ASY, Re,

412   and Ri at 550 nm wavelength for Asian PDU are 0.935±0.014, 0.742±0.008,

413   1.526±0.029, and 0.00226±0.00056, respectively, while corresponding values are

414   0.921±0.021, 0.723±0.009, 1.521±0.025, 0.00364±0.0014 for TDU. Yang et al. (2009)

415   took advantage of various in situ aerosol optical and chemical measurements at

416   Xianghe, China during the EAST-AIRC campaign, and deduced a refractive index of

417   1.53-0.0023i at 550 nm of dust aerosol, which is close to the result of PDU in this

418   study. Nevertheless, the TDU case should be much closer to actual airborne dust

419   aerosol in the real world. When the elevated dusts over desert source regions are

420   transported eastward, they generally mix with other chemical species and react

421   heterogeneously with anthropogenic pollutants, and thus may significantly modify

422   their chemical composition and microphysical properties (Arimoto et al., 2004).

423   Recently, Kim et al. (2011) presented that the annual mean SSA, ASY, Re, and Ri of

424   complex refractive index for nearly pure Saharan dust are 0.944±0.005, 0.752±0.014,

425   1.498±0.032, and 0.0024±0.0034 at 550 nm, respectively, which are close to our

426   results of pure Asian dust but exist some differences of quantitative values and

427   spectral behaviors.

428   Average spectral optical properties (at 440, 675, 870, and 1020 nm) for PDU and

429   TDU over East and Central Asian regions are tabulated in Table 2. To our knowledge,

430   this is the first built on Asian dust optical characteristics utilizing multiyear and

431   multi-site AERONET measurements, which will hopefully improve uncertainties of

432   Asian dust shortwave radiative forcing in current regional and global climate models.

433 **4. Discussion**

434   Figure 8 describes the mean spectral behaviors of Re, RI, and SSA for Asian Pure

435   Dust (α<0.2) in this study along with published dust results over various geographical

436   locations (Carlson and Caverly, 1977 or C77; Patterson et al., 1977 or P77; WMO,

437   1983; Hess et al., 1998 or OPAC; Dubovik et al., 2002b or Persian Gulf; Alfaro et al.,

438   2004 or Ulan Buh Desert; Wang et al., 2004 or ADEC; Todd et al., 2007 or T07). It is

439   well known that a lot of present-day dust models commonly take advantage of the

440   Optical Properties of Aerosols and Clouds (OPAC, Hess et al., 1998) or World

441   Meteorological Organization (WMO, 1983) databases. Curves C77 and P77 show the

442   complex refractive index of Saharan dust in Cape Verde Islands, Barbados West

443   Indies, Tenerife Canary Islands obtained from laboratory analysis by Carlson and

444   Caverly (1977) and Patterson et al. (1977), respectively. Curve P77 gives one of the

most widely used datasets of Ri value in the range 300-700 nm. Curve Persian

Gulf(98-00) displays the refractive index and SSA of dust over Bahrain-Persian Gulf

Desert during period of 1998-2000 derived from Dubovik et al. (2002b). Curve T07

shows the optical properties of mineral dust over Bodélé Depression of northern Chad

during 2005 retrieved from Cimel sun photometer by Todd et al. (2007). And the

curves ADEC and Ulan Buh exhibit the dust absorptive properties over

aforementioned Taklimakan Desert and Ulan Buh Desert of northwest China by Wang

et al. (2004) and Alfaro et al. (2004). Figure 8(a) presents that the spectral behaviors

of Re have relatively slight variations with values ranging from 1.50-1.56 apart from

T07 that shows lower Re values of 1.44-1.47. Todd et al. (2007) utilized Scanning

Electron Microscope (SEM) analysis of airborne dust material and confirmed that the

mineral dust is dominated by fragmented fossil diatoms from the dry lake bed of the

Bodélé Depression, which is to some extent different from the typical desert soil. As

shown in Figure 8(b), wavelength dependences of Ri exhibit comparably greater

differences in UV wavebands. In mid-visible and near infrared, our results are slightly

larger than Persian Gulf (98-00) and T07 that are retrieved from Cimel sun

photometer, but still comparable. It is very distinct that the absorbing ability of Asian

pure dust ($\alpha<0.2$) in the whole spectrum range is about a factor of 4 smaller than

current dust models (WMO, 1983; Hess et al., 1998), and is a factor of 2 to 3 lower

than the results from in situ measurements combined with laboratory analysis or

model calculations (Carlson and Caverly, 1977; Patterson et al., 1977; Wang et al.,

2004). Meanwhile, the wavelength dependences of SSA agree well with Persian Gulf

(98-00) and Ulan Buh Desert, but are much higher than OPAC. The discrepancy

increases dramatically with decreasing wavelength. Such big differences of dust

absorption capacity for diverse dust models (OPAC and WMO) and researches will

certainly lead to different radiative impacts on regional or global climate change.

Figure 9 draws the aerosol shortwave direct radiative effects (ARF) at the top of

atmosphere (TOA), at the surface (SFC), and in the atmospheric layer (ATM) for

Asian Pure Dust ($\alpha<0.2$) and Transported Anthropogenic Dust ($0.2<\alpha<0.6$) acquired

in this study, and corresponding ARF values for OPAC Mineral accumulated (Mineral

acc.) and transported (Mineral tran.) modes are also presented for comparison. We make use of the Santa Barbara Discrete-ordinate Atmospheric Radiative Transfer model (SBDART, Ricchiazzi et al., 1998) to calculate the ARF, which has been proved to be a reliable software code and widely used for simulating plane-parallel radiative fluxes in the Earth's atmosphere (Halthore et al., 2005; Bi et al., 2013). The main input parameters of spectral AOD, surface albedo, WVC, and columnar ozone amount are prescribed to same values (e.g., 0.72, 0.30, 1.0 cm, and 300 DU for input AOD_{440}, surface albedo, WVC, and ozone amount), and the spectral SSA, ASY, Re, and Ri values are obtained from aforementioned various dust models. It is evident that Earth's energy budget is modulated and redistributed by different absorbing properties of mineral dusts. The results indicate that the cooling rate at SFC (negative radiative forcing) gradually increases with PDU ($\alpha<0.2$), TDU ($0.2<\alpha<0.6$), OPAC Mineral accumulated and transported dust modes. By contrast, the cooling intensity at TOA gradually decreases with diverse dust cases, and even becomes positive radiative forcing for OPAC transported dust mode, with ARF varying from -15.6, -13.8, -6.9, and +0.24 Wm^{-2}, respectively. Therefore, the heating intensity in the atmospheric layer sharply increases from +22.7, +29.5, +46.6, and +58.3 Wm^{-2}. The heating rate in ATM for OPAC Mineral (acc. and tran.) modes is about two-fold greater than Asian dust cases (PDU and TDU). Such large diabatic heating rates might warm the dust layer, suppress the development of convection under the lower atmosphere, thus exert profound impacts on the atmospheric dynamical and thermodynamic structures and cloud formation together with the strength and occurrence frequency of precipitation (Rosenfeld et al., 2001; Huang et al., 2010a; Creamean et al., 2013). Hence, accurate and reliable absorbing characteristics of Asian dust should be considered in present-day regional climate models.

5. Summary

In this study, we have proposed two threshold criteria to discriminate two types of Asian dust: Pure Dust (PDU, $\alpha<0.2$) and Transported Anthropogenic Dust (TDU, $0.2<\alpha<0.6$). PDU can represent nearly "pure" dust in desert source regions and

decrease disturbance of other non-dust aerosols, which would also exclude some fine mode of dust particles. The spectral behaviors of TDU exhibit similar variations with PDU, but show much stronger absorption and weaker scattering than PDU cases. There are two markedly identifiable characteristics for Asian PDU. (I) spectral SSA values systematically increase with wavelength from 440 nm to 675 nm and remain almost neutral or slight increase for the wavelength greater than 675 nm, whereas an opposite pattern is shown for imaginary part of refractive index. (II) Asian pure dust aerosols have got AE values smaller than 0.2 and AAE larger than 1.50. Compared with current common dust models (e.g., OPAC and WMO), Asian dust aerosol has relatively weak absorption for wavelengths greater than 550 nm (SSA~0.96-0.99), but presents a moderate absorption in the blue spectral range (SSA$_{440}$~0.92-0.93). The overall average values of SSA, ASY, Re, and Ri at 550 nm wavelength for Asian PDU are 0.935±0.014, 0.742±0.008, 1.526±0.029, and 0.00226±0.00056, respectively, while corresponding values are 0.921±0.021, 0.723±0.009, 1.521±0.025, 0.00364±0.0014 for TDU.

It should be noted that the definition of anthropogenic dust in this paper is ambiguous, and TDU here represents more accurately dominant dust mixing with other anthropogenic aerosols. It is very difficult to quantify the anthropogenic contribution due to large uncertainties in defining the anthropogenic fraction of ambient dust burden (Sokolik et al., 2001; Huang et al., 2015). Diverse human activities (e.g., agricultural cultivation, desertification, industrial activity, transportation, and construction in urbanization) in vulnerable environments might modify the land use and Earth's surface cover, and would affect the occurred frequency and intensity of anthropogenic dust. Hence, the optical features of anthropogenic dust aerosols are dependent on the source regions and chemical compositions. However, as concluded by Huang et al. (2015), anthropogenic dust generated by human activities mainly comes from semi-arid and semi-humid regions (Guan et al., 2016) and is generally mixed with other types of aerosols within the PBL. And we primarily investigated dust aerosols in arid or semi-arid regions over East and Central Asia, where are somewhat disturbed by human activities. Therefore, the key

optical properties of TDU derived from this study should to some extent contain the anthropogenic fraction. To fully elucidate exact optical properties of anthropogenic dust, we need to explore detailed morphology, mineralogy, and chemical compositions by means of in situ measurements, laboratory analysis, active and passive remote sensing methods (e.g., multi-wavelength lidar, AEROENT, MODIS) as well as model calculations.

Acknowledgements. This work was jointly supported by the National Science Foundation of China (41521004, 41305025, 41575015 and 41405113), the Fundamental Research Funds for the Central Universities lzujbky-2015-4 and lzujbky-2016-k01, and the China 111 Project (No. B 13045). We thank the GSFC/NASA AERONET group for processing the AERONET data (http://aeronet.gsfc.nasa.gov). The authors would like to express special thanks to the principal investigators (Hong-Bin Chen, Philippe Goloub, Bernadette Chatenet, Xiao-Ye Zhang, Laurent Gomes, Sabur F. Abdullaev, and Hamid Khalesifard) and their staff for effort in establishing and maintaining the instruments at AERONET sites used in this work. We appreciate the MODIS and TOMS teams for supplying the satellite data. We would also like to thank all anonymous reviewers for their constructive and insightful comments.

References

Alam, K., Trautmann, T., and Blaschke, T.: Aerosol optical properties and radiative forcing over mega-city Karachi, Atmos. Res., 101, 773-782, doi:10.1016/j.atmosres.2011.05.007, 2011.

Alfaro, S. C., Lafon, S., Rajot, J. L., Formenti, P., Gaudichet, A., and Maillé, M.: Iron oxides and light absorption by pure desert dust: An experimental study, J. Geophys. Res., 109, D08208, doi:10.1029/2003JD004374, 2004.

Alizadeh Choobari, O., Zawar-Reza, P., and Sturman, A.: The global distribution of mineral dust and its impacts on the climate system: A review, Atmos. Res., 138, 152-165, doi:10.1016/j.atmosres.2013.11.007, 2014.

Aoki, T., Motoyoshi, H., Kodama, Y., Yasunari, T. J., Sugiura, K., and Kobayashi, H.: Atmospheric aerosol deposition on snow surfaces and its effect on albedo, SOLA, 2, 13-16,

doi:10.2151/sola.2006-004, 2006.

Arimoto, R., X. Y. Zhang, B .J. Huebert, C. H. Kang, D. L. Savoie, J. M. Prospero, S. K. Sage, C. A. Schloesslin, H. M. Khaing, and S. N. Oh: Chemical composition of atmospheric aerosols from Zhenbeitai, China, and Gosan, South Korea, during ACE-Asia, J. Geophys. Res., 109, D19S04, doi:10.1029/2003JD004323, 2004.

Bi, J., Huang, J., Fu, Q., Wang, X., Shi, J., Zhang, W., Huang, Z., and Zhang B.: Toward characterization of the aerosol optical properties over Loess Plateau of Northwestern China, J. Quant. Spectrosc. Radiat. Transfer., 112, 346-360, doi:10.1016/j.jqsrt.2010.09.006, 2011.

Bi, J., Huang, J., Fu, Q., Ge, J., Shi, J., Zhou, T., and Zhang, W.: Field measurement of clear-sky solar irradiance in Badain Jaran Desert of Northwestern China, J. Quant. Spectroc. Radiat. Transf., 122, 194-207, doi:10.1016/j.jqsrt.2012.07.025, 2013.

Bi, J., Shi, J., Xie, Y., Liu, Y., Takamura, T., and Khatri, P.: Dust aerosol characteristics and shortwave radiative impact at a Gobi Desert of Northwest China during the spring of 2012. J. Meteo. Soc. Jp, 92A, 33-56, DOI:10.2151/jmsj.2014-A03, 2014.

Carlson, T. N. and Caverly, R. S.: Radiative characteristics of Saharan dust at solar wavelengths, J. Geophys. Res., 82(21), 3141-3152, 1977.

Chan, C. -C., Chuang, K. -J., Chen, W. -J., Chang, W. -T., Lee, C. -T., and Peng, C. -M.: Increasing cardiopulmonary emergency visits by long-range transported Asian dust storms in Taiwan, Environ. Res., 106, 393-400, 2008.

Charlson, R. J., Schwartz, S. E., Hales, J. M., Cess, R. D., Coakley Jr., J. A., Hansen, J. E., and Hofmann, D. J.: Climate forcing by anthropogenic aerosols, Science, 255, 423-430, doi:10.1126/science.255.5043.423, 1992.

Che, H., Shi, G., Uchiyama, A., Yamazaki, A., Chen, H., Goloub, P., and Zhang, X.: Intercomparison between aerosol optical properties by a PREDE skyradiometer and CIMEL sunphotometer over Beijing, China, Atmos. Chem. Phys., 8, 3199-3214, doi:10.5194/acp-8-3199-2008, 2008.

Che, H., et al.: Instrument calibration and aerosol optical depth validation of the China Aerosol Remote Sensing Network, J. Geophys. Res., 114, D03206, doi:10.1029/2008JD011030, 2009a.

Che, H., Zhang, X., Alfraro, S., Chatenet, B., Gomes, L., and Zhao, J.: Aerosol optical properties and its radiative forcing over Yulin, China in 2001 and 2002, Adv. Atmos. Sci., 26(3), 564-576,

593   doi:10.1007/s00376-009-0564-4, 2009b.

594   Che, H., Wang, Y., Sun, J., Zhang, X., Zhang, X., and Guo, J.: Variation of aerosol optical

595   properties over the Taklimakan Desert in China, Aerosol Air Qual. Res., 13, 777-785,

596   doi:10.4209/aaqr.2012.07.0200, 2013.

597   Che, H., Xia, X., Zhu, J., Li, Z., Dubovik, O., Holben, B., Goloub, P., Chen, H., Estelles, V.,

598   Cuevas-Agulló, E., Blarel, L., Wang, H., Zhao, H., Zhang, X., Wang, Y., Sun, J., Tao, R., Zhang,

599   X., and Shi, G.: Column aerosol optical properties and aerosol radiative forcing during a serious

600   haze-fog month over North China Plain in 2013 based on ground-based sunphotometer

601   measurements, Atmos. Chem. Phys., 14, 2125-2138, doi:10.5194/acp-14-2125-2014, 2014.

602   Che, H., Zhang, X.-Y., Xia, X., Goloub, P., Holben, B., Zhao, H., Wang, Y., Zhang, X.-C., Wang,

603   H., Blarel, L., Damiri, B., Zhang, R., Deng, X., Ma, Y., Wang, T., Geng, F., Qi, B., Zhu, J., Yu,

604   J., Chen, Q., and Shi, G.: Ground-based aerosol climatology of China: aerosol optical depths

605   from the China Aerosol Remote Sensing Network (CARSNET) 2002–2013, Atmos. Chem.

606   Phys., 15, 7619-7652, doi:10.5194/acp-15-7619-2015, 2015.

607   Chin, M., Diehl, T., Dubovik, O., Eck, T. F., Holben, B. N., Sinyuk, A., and Streets, D. G.: Light

608   absorption by pollution, dust, and biomass burning aerosols: a global model study and

609   evaluation with AERONET measurements, Ann. Geophys., 27, 3439-3464,

610   doi:10.5194/angeo-27-3439-2009, 2009.

611   Claquin, T., Schulz, M., Balkanski, Y., and Boucher, O.: Uncertainties in assessing radiative

612   forcing by mineral dust, Tellus Ser. B, 50, 491-505, 1998.

613   Claquin, T., Schulz, M., and Balkanski, Y.: Modeling the mineralogy of atmospheric dust sources,

614   J. Geophys. Res., 104, D18, 22243-22256, 1999.

615   Creamean, J. M., Suski, K. J., Rosenfeld, D., Cazorla, A., DeMott, P. J., Sullivan, R. C., White, A.

616   B., Ralph, F. M., Minnis, P., Comstock, J. M., Tomlinson, J. M., and Prather, K. A.: Dust and

617   biological aerosols from the Sahara and Asia influence precipitation in the western U.S.,

618   Science, 339, 1572-1578, doi:10.1126/science.1227279, 2013.

619   DeMott, P. J., Sassen, K., Poellot, M. R., Baumgardner, D., Rogers, D. C., Brooks, S. D., Prenni,

620   A. J., and Kreidenweis, S. M.: African dust aerosols as atmospheric ice nuclei, Geophys. Res.

621   Lett., 30(14), 1732, doi:10.1029/2003GL017410, 2003.

622   Dubovik, O. and King, M. D.: A flexible inversion algorithm for retrieval of aerosol optical

623   properties from Sun and sky radiance measurements, J. Geophys. Res., 105(D16),

624   20673-20696,

625 doi:10.1029/2000JD900282, 2000.

626 Dubovik, O., Smirnov, A., Holben, B. N., King, M. D., Kaufman, Y. J., Eck, T. F., and Slutsker, I.:

627   Accuracy assessments of aerosol optical properties retrieved from Aerosol Robotic Network

628   (AERONET) Sun and sky radiance measurements, J. Geophys. Res., 105(D8), 9791–9806,

629   doi:10.1029/2000JD900040, 2000.

630 Dubovik, O., Holben, B. N., Lapyonok, T., Sinyuk, A., Mishchenko, M. I., Yang, P., and Slutsker,

631   I.: Non-spherical aerosol retrieval method employing light scattering by spheroids, Geophys.

632   Res. Lett., 29(10), 1415, doi:10.1029/2001GL014506, 2002a.

633 Dubovik, O., Holben, B. N., Eck, T. F., Smirnov, A., Kaufman, Y. J., King, M. D., Tanré, D., and

634   Slutsker, I.: Variability of absorption and optical properties of key aerosol types observed in

635   worldwide locations, J. Atmos. Sci., 59, 590–608, 2002b.

636 Dubovik, O., Sinyuk, A., Lapyonok, T. Holben, B. N., Mishchenko, M., Yang, P., Eck, T. F.,

637   Volten, H., Muñoz, O., Veihelmann, B., van der Zande, W. J., Leon, J. –F., Sorokin, M., and

638   Slutsker, I.: Application of spheroid models to account for aerosol particle nonsphericity in

639   remote sensing of desert dust, J. Geophys. Res., 111, D11208, doi:10.1029/2005JD006619,

640   2006.

641 Eck, T. F., Holben, B. N., Reid, J. S., Dubovik, O., Smirnov, A., O'Neill, N. T., Slutsker, I., and

642   Kinne, S.: Wavelength dependence of the optical depth of biomass burning, urban and desert

643   dust aerosols, J. Geophys. Res., 104, 31 333-31350, 1999.

644 Eck, T. F., et al.: Columnar aerosol optical properties at AERONET sites in central eastern Asia

645   and aerosol transport to the tropical mid-Pacific, J. Geophys. Res., 110, D06202,

646   doi:10.1029/2004JD005274, 2005.

647 Fu, Q., Thorsen, T., Su, J., Ge, J., and Huang, J.: Test of Mie-based single-scattering properties of

648   non-spherical dust aerosols in radiative flux calculations, J. Quant. Spectroc. Radiat. Transf.,

649   110, 1640-1653, doi:10.1016/j.jqsrt.2009.03.010, 2009.

650 Ge, J., Su, J., Ackerman, T. P., Fu, Q., Huang, J., and Shi, J.: Dust aerosol optical properties

651   retrieval and radiative forcing over northwest China during the 2008 China-U.S. joint field

652   experiment, J. Geophys. Res., 115, D00K12, doi:10.1029/2009JD013263, 2010.

653 Ginoux, P., Prospero, J. M., Gill, T. E., Hsu, N. C., and Zhao, M.: Global-scale attribution of

654   anthropogenic and natural sources and their emission rates based on MODIS Deep Blue aerosol

655   products, Rev. Geophys., 50, RG3005, doi:10.1029/2012RG000388, 2012.

656 Golitsyn, G. and Gillette, D. A.: Introduction: A joint Soviet-American experiment for the study of

657   Asian desert dust and its impact on local meteorological conditions and climate, Atmos.

658   Environ., 27A, 16, 2467-2470, 1993.

659 Guan X., Huang, J., Guo, N., Bi, J., and Wang, G.: Variability of soil moisture and its relationship

660   with surface albedo and soil thermal parameters over the Loess Plateau, Adv. Atmos. Sci., 26(9),

661   692-700, doi:10.1007/s00376-009-8198-0, 2009.

662 Guan, X., Huang, J., Zhang, Y., Xie, Y., and Liu, J.: The relationship between anthropogenic dust

663   and population over global semi-arid regions, Atmos. Chem. Phys., 16, 5159-5169,

664   doi:10.5194/acp-16-5159-2016, 2016.

665 Halthore, R. N., et al.: Intercomparison of shortwave radiative transfer codes and measurements, J.

666   Geophys. Res., 110, D11206, doi:10.1029/2004JD005293, 2005.

667 Hansen, J., Sato, M., and Ruedy, R.: Radiative forcing and climate response, J. Geophys. Res., 102,

668   6831-6864, 1997.

669 Hess, M., Kopke, P., and Schult, I.: Optical properties of aerosols and clouds: The software

670   package OPAC, Bull. Amer. Meteor. Soc., 79, 831-844, 1998.

671 Holben, B. N., Eck, T. F., Slutsker, I., Tanre, D., Buis, J. P., Setzer, A., Vermote, E., Reagan, J. A.,

672   Kaufman, Y. J., Nakajima, T., Lavenu, F., Jankowiak, F., and Smirnov, A., AERONET—A

673   federated instrument network and data archive for aerosol characterization, Remote Sens.

674   Environ., 66, 1-16, 1998.

675 Huang, J., Minnis, P., Lin, B., Yi, Y., Khaiyer, M. M., Arduini, R. F., Fan, A., and Mace, G. G.:

676   Advanced retrievals of multilayered cloud properties using multispectral measurements, J.

677   Geophys. Res., 110, D15S18, doi:10.1029/2004JD005101, 2005.

678 Huang, J., Lin, B., Minnis, P., Wang, T., Wang, X., Hu, Y., Yi, Y., and Ayers, J. K.: Satellite-based

679   assessment of possible dust aerosols semi-direct effect on cloud water path over East Asia,

680   Geophys. Res. Lett., 33, L19802, doi:10.1029/2006GL026561, 2006.

681 Huang, J., Minnis, P., Chen, B., Huang, Z., Liu, Z., Zhang, Q., Yi, Y., and Ayers, J. K.: Long-range

682   transport and vertical structure of Asian dust from CALIPSO and surface measurements during

683   PACDEX, J. Geophys. Res., 113, D23212, doi:10.1029/2008JD010620, 2008a.

684   Huang, J., Zhang, W., Zuo, J., Bi, J., Shi, J., Wang, X., Chang, Z., Huang, Z., Yang, S., Zhang, B.,

685   Wang, G., Feng, G., Yuan, J., Zhang, L., Zuo, H., Wang, S., Fu, C., and Chou, J.: An overview of

686   the semi-arid climate and environment research observatory over the Loess Plateau, Adv. Atmos.

687   Sci., 25, 906-921, doi:10.1007/s00376-008-0906-7, 2008b.

688   Huang, J., Fu, Q., Su, J., Tang, Q., Minnis, P., Hu, Y., Yi, Y., and Zhao, Q.: Taklimakan dust

689   aerosol radiative heating derived from CALIPSO observations using the Fu-Liou radiation

690   model   with   CERES   constraints,   Atmos.   Chem.   Phys.,   9,   4011-4021,

691   doi:10.5194/acp-9-4011-2009, 2009.

692   Huang, J., Minnis, P., Yan, H., Yi, Y., Chen, B., Zhang, L., and Ayers, J. K.: Dust aerosol effect on

693   semi-arid climate over Northwest China detected from A-Train satellite measurements, Atmos.

694   Chem. Phys., 10, 6863-6872, doi:10.5194/acp-10-6863-2010, 2010a.

695   Huang, J., Fu, Q., Zhang, W., Wang, X., Zhang, R., Ye, H., and Warren, S. G.: Dust and black

696   carbon in seasonal snow across northern China, Bull. Amer. Meteor. Soc., 92, 175-181,

697   doi:10.1175/2010BAMS3064.1, 2011.

698   Huang, J., Wang, T., Wang, W., Li, Z., and Yan, H.: Climate effects of dust aerosols over East

699   Asian   arid   and   semiarid   regions,   J.   Geophys.   Res.,   119,   11398-11416,

700   doi:10.1002/2014JD021796, 2014.

701   Huang, J. P., Liu, J. J., Chen, B., and Nasiri, S. L.: Detection of anthropogenic dust using

702   CALIPSO   lidar   measurements,   Atmos.   Chem.   Phys.,   15,   11653-11665,

703   doi:10.5194/acp-15-11653-2015, 2015.

704   Huang, J., Yu, H., Guan, X., Wang, G., and Guo, R.: Accelerated dryland expansion under climate

705   change, Nature Clim. Change, 6(2), 166-171, doi:10.1038/nclimate2837, 2016.

706   Huang, Z., Huang, J., Bi, J., Wang, G., Wang, W., Fu, Q., Li, Z., Tsay, S.-C., and Shi, J.: Dust

707   aerosol vertical structure measurements using three MPL lidars during 2008 China-U.S. joint

708   dust field experiment, J. Geophys. Res., 115, D00K15, doi:10.1029/2009JD013273, 2010b.

709   Huebert, B. J., Bates, T., Russell, P. B., Shi, G., Kim, Y. J., Kawamura, K., Carmichael, G., and

710   Nakajima, T.: An overview of ACE-Asia: Strategies for quantifying the relationships between

711   Asian   aerosols   and   their   climatic   impacts,   J.   Geophys.   Res.,   108(D23),   8633,

712   doi:10.1029/2003JD003550, 2003.

713 Husar, R. B., Tratt, D. M., and Schichtel, B. A., et al.: Asian dust events of April 1998, J. Geophys.

714   Res., 106, D16, 18317-18330, 2001.

715 Jickells, T., An, Z., Andersen, K., Baker, A., Bergametti, G., Brooks, N., Cao, J., Boyd, P., Duce,

716   R., Hunter, K., Kawahata, H., Kubilay, N., laRoche, J., Liss, P., Mahowald, N., Prospero, J.,

717   Ridgwell, A., Tegen, I., and Torres, R.: Global iron connections between desert dust, ocean

718   biogeochemistry, and climate, Science, 308, 67-71, doi:10.1126/science.1105959, 2005.

719 Kim, D.-H., Sohn, B. -J., Nakajima, T., Takamura, T., Takemura, T., Choi, B. -C., and Yoon, S. -C.:

720   Aerosol optical properties over east Asia determined from ground-based sky radiation

721   measurements, J. Geophys. Res., 109, D02209, doi:10.1029/2003JD003387, 2004.

722 Kim, D., Chin, M., Yu, H., Eck, T. F., Sinyuk, A., Smirnov, A., and Holben, B. N.: Dust optical

723   properties over North Africa and Arabian Peninsula derived from the AERONET dataset, Atmos.

724   Chem. Phys., 11, 10733-10741, doi:10.5194/acp-11-10733-2011, 2011.

725 Kinne, S., Schulz, M., Textor, C., Guibert, S., Balkanski, Y., Bauer, S. E., Berntsen, T., Berglen, T.

726   F., Boucher, O., Chin, M., Collins, W., Dentener, F., Diehl, T., Easter, R., Feichter, J., Fillmore,

727   D., Ghan, S., Ginoux, P., Gong, S., Grini, A., Hendricks, J., Herzog, M., Horowitz, L., Isaksen,

728   I., Iversen, T., Kirkevåg, A., Kloster, S., Koch, D., Kristjansson, J. E., Krol, M., Lauer, A.,

729   Lamarque, J. F., Lesins, G., Liu, X., Lohmann, U., Montanaro, V., Myhre, G., Penner, J., Pitari,

730   G., Reddy, S., Seland, O., Stier, P., Takemura, T., and Tie, X.: An AeroCom initial assessment –

731   optical properties in aerosol component modules of global models, Atmos. Chem. Phys., 6,

732   1815-1834, doi:10.5194/acp-6-1815-2006, 2006.

733 Lafon, S., Rajot, J.-L., Alfaro, S. C., and Gaudichet, A.: Quantification of iron oxides in desert

734   aerosol, Atmos. Environ., 38, 1211-1218, 2004.

735 Lafon, S., Sokolik, I. N., Rajot, J. L., Caquineau, S., and Guadichet, A.: Characterization of iron

736   oxides in mineral dust aerosols: Implications for light absorption, J. Geophys. Res., 111,

737   D21207, doi:10.1029/2005JD007016, 2006.

738 Li, Z., Li, C., Chen, H., Tsay, S.-C., Holben, B., Huang, J., Li, B., Maring, H., Qian, Y., Shi, G.,

739   Xia, X., Yin, Y., Zheng, Y., and Zhuang, G.: East Asian Studies of Tropospheric Aerosols and

740   their Impact on Regional Climate (EAST-AIRC): An overview, J. Geophys. Res., 116, D00K34,

741   doi:10.1029/2010JD015257, 2011.

742 Mikami, M., Shi, G. Y., Uno, I., Yabuki, S., Iwasaka, Y., Yasui, M., Aoki, T., Tanaka, T. Y.,

Kurosaki, Y., Masuda, K., Uchiyama, A., Matsuki, A., Sakai, T., Takemi, T., Nakawo, M., Seino, N., Ishizuka, M., Satake, S., Fujita, K., Hara, Y., Kai, K., Kanayama, S., Hayashi, M., Du, M., Kanai, Y., Yamada, Y., Zhang, X. Y., Shen, Z., Zhou, H., Abe, Q., Nagai, T., Tsutsumi, Y. , Chiba, M., and Suzuki, J.: Aeolian dust experiment on climate impact: An overview of Japan-China joint project ADEC, Global Planet. Change, 52, 142-172, doi:10.1016/j.gloplacha.2006.03.001, 2006.

Morman, S. A. and Plumlee, G. S.: The role of airborne mineral dusts in human disease, Aeolian Res., 9, 203-212, 2013.

Nakajima, T., Tonna, G., Rao, R., Boi, P., Kaufman, Y., and Holben, B.: Use of sky brightness measurements from ground for remote sensing of particulate polydispersions, Appl. Opt., 35(15), 2672-2686, doi:10.1364/AO.35.002672, 1996.

Nakajima, T., Sekiguchi, M., Takemura, T., Uno, I., Higurashi, A., Kim, D., Sohn, B. J., Oh, S. -N., Nakajima, T. Y., Ohta, S., Okada, I., Takamura, T, and Kawamoto, K.: Significance of direct and indirect radiative forcings of aerosols in the East China Sea region, J. Geophys. Res., 108(D23), 8658, doi:10.1029/2002JD003261, 2003.

Okin, G. S., Mahowald, N., Chadwick, O. A., and Artaxo, P.: Impact of desert dust on the biogeochemistry of phosphorus in terrestrial ecosystems, Global Biogechem. Cycles, 18, GB2005, doi:10.1029/2003GB002145, 2004.

Pandithurai, G., Dipu, S., Dani, K. K., Tiwari, S., Bisht, D. S., Devara, P. C. S., and Pinker, R. T.: Aerosol radiative forcing during dust events over New Delhi, India, J. Geophys. Res., 113, D13209, doi:10.1029/2008JD009804, 2008.

Patterson, E. M., Gillette, D. A., and Stockton, B.: Complex index of refraction between 300 and 700 nm for Saharan aerosols, J. Geophys. Res., 82(21), 3153-3160, 1977.

Perlwitz, J., Tegen, I., and Miller, R. L.: Interactive soil dust aerosol model in GISS GCM, 1. Sensitivity of the soil dust cycle to radiative properties of soil dust aerosols, J. Geophys. Res., 106, D16, 18167-18192, 2001.

Prospero, J. M., Ginoux, P., Torres, O., Nicholson, S. E., and Gill, T. E.: Environmental characterization of global sources of atmospheric soil dust identified with the Nimbus 7 total ozone mapping spectrometer (TOMS) absorbing aerosol product, Rev. Geophys., 40(1), 1002, doi:10.1029/2000RG000095, 2002.

773   Ramanathan, V., Crutzen, P. J., Kiehl, J. T., and Rosenfeld, D.: Aerosols, climate, and the

774   hydrological cycle, Science, 294, 2119-2124, doi:10.1126/science.1064034, 2001.

775   Ricchiazzi, P., Yang, S., Gautier, C., and Sowle, D.: SBDART: A research and teaching software

776   tool for plane-parallel radiative transfer in the Earth's atmosphere, Bull. Amer. Meteor. Soc., 79,

777   2101-2114, 1998.

778   Rosenfeld, D., Rudich, Y., and Lahav, R.: Desert dust suppressing precipitation: A possible

779   desertification feedback loop, Proc. Natl. Acad. Sci. U.S.A., 98, 5975-5980, 2001.

780   Shao, Y., Wyrwoll, K.-H., Chappel, A., Huang, J., Lin, Z., McTainsh, G., Mikami, M., Tanaka, T.,

781   Wang, X., and Yoon, S.: Dust cycle: An emerging core theme in Earth system science, Aeolian

782   Res., 2, 181-204, 2011.

783   Shen, Z., Sun, J., Cao, J., Zhang, L., Zhang, Q., Lei, Y., Gao, J., Huang, R., Liu, S., Huang, Y.,

784   Zhu, C., Xu, H., Zheng, C., Liu, P., and Xue, Z.: Chemical profiles of urban fugitive dust PM2.5

785   samples in Northern Chinese cities, Sci. Total Environ., 569-570, 619-626,

786   doi:10.1016/j.scitotenv.2016.06.156, 2016.

787   Smirnov, A., Holben, B. N., Eck, T. F., Dubovik, O., and Slutsker, I.: Cloud screening and quality

788   control algorithms for the AERONET database, Remote Sens. Environ., 73, 337-349, 2000.

789   Smirnov, A., Holben, B. N., Kaufman, Y. J., Dubovik, O., Eck, T. F., Slutsker, I., Pietras, C., and

790   Halthore, R.: Optical properties of atmospheric aerosol in maritime environments, J. Atmos.

791   Sci., 59, 501-523, 2002.

792   Sokolik, I. N. and Golitsyn, G.: Investigation of optical and radiative properties of atmospheric

793   dust aerosols, Atmos. Environ., 27A, 16, 2509-2517, 1993.

794   Sokolik, I. N. and Toon, O. B.: Incorporation of mineralogical composition into models of the

795   radiative properties of mineral aerosol from UV to IR wavelengths, J. Geophys. Res., 104, D8,

796   9423-9444, 1999.

797   Sokolik, I. N., Winker, D. M., Bergametti, G., Gillette, D. A., Garmichael, G., Kaufman, Y. J.,

798   Gomes, L., Schuetz, L., and Penner, J. E.: Introduction to special section: Outstanding problems

799   in quantifying the radiative impacts of mineral dust, J. Geophys. Res., 106, D16, 18015-18027,

800   2001.

801   Takamura, T., Nakajima, T., and SKYNET community group: Overview of SKYNET and its

802   Activities, Opt. Puray Apl., 37, 3303-3308, 2004.

803   Tegen, I. and Fung, I.: Contribution to the atmospheric mineral aerosol load from land surface

804   modification, J. Geophys. Res., 100, 18707-18726, doi:10.1029/95JD02051, 1995.

805   Todd, M. C., Washington, R., Martins, J. V., Dubovik, O., Lizcano, G., M'Bainayel, S., and

806   Engelstaedter, S.: Mineral dust emission from the Bodélé Depression, northern Chad, during

807   BoDEx 2005, J. Geophys. Res., 112, D06207, doi:10.1029/2006JD007170, 2007.

808   Uchiyama, A., Yamazaki, A., Togawa, H., Asano, J., and Shi, G.-Y.: Single scattering albedo of

809   Aeolian dust as inferred from sky-radiometer and in situ ground-based measurement, SOLA,

810   Vol. 1, pp. 209-212, doi:10.2151/sola.2005-054, 2005.

811   Uno, I., Eguchi, K., Yumimoto, K., Takemura, T., Shimizu, A., Uematsu, M., Liu, Z., Wang, Z.,

812   Hara, Y., and Sugimoto, N.: Asian dust transported one full circuit around the globe, Nature

813   Geosci., 2, 557-560, doi:10.1038/NGEO583, 2009.

814   Uno,I., Eguchi, K., Yumimoto, K., Liu, Z., Hara, Y., Sugimoto, N., Shimizu, A., and Takemura, T.:

815   Large Asian dust layers continuously reached North America in April 2010, Atmos. Chem.

816   Phys., 11, 7333-7341, 2011.

817   Wang, G., Huang, J., Guo, W., Zuo, J., Wang, J., Bi, J., Huang, Z., and Shi, J.: Observation

818   analysis of land-atmosphere interactions over the Loess Plateau of northwest China, J. Geophys.

819   Res., 115, D00K17,doi:10.1029/2009JD013372, 2010a.

820   Wang, H., Shi, G. Y., Aoki, T., Wang, B., and Zhao, T. L.: Radiative forcing due to dust aerosol

821   over east Asia-north Pacific region during spring, 2001, Chin. Sci. Bull., 49(20): 2212-2219,

822   2004.

823   Wang, H., Zhang, X., Gong, S., Chen, Y., Shi, G., and Li, W.: Radiative feedback of dust aerosols

824   on the East Asian dust storms, J. Geophys. Res., 115, D23214, doi:10.1029/2009JD013430,

825   2010b.

826   Wang, W., Huang, J., Minnis, P., Hu, Y., Li, J., Huang, Z., Ayers, J. K., and Wang, T.: Dusty cloud

827   properties and radiative forcing over dust source and downwind regions derived from A-Train

828   data during the Pacific Dust Experiment, J. Geophys. Res., 115, D00H35,

829   doi:10.1029/2010JD014109, 2010c.

830   Wang, X., Huang, J., Ji, M., and Higuchi, K.: Variability of East Asia dust events and their

831   long-term trend, Atmos. Environ., 42, 13, 3156-3165, doi:10.1016/j.atmosenv.2007.07.046,

832   2008.

833   Wang, X., Doherty, S. J., and Huang, J.: Black carbon and other light-absorbing impurities in

834   snow across Norhtern China, J. Geophys. Res., 118, 1471-1492, doi:10.1029/2012JD018291,

835   2013.

836   Wang, X., Pu, W., Shi, J., Bi, J., Zhou, T., Zhang, X., and Ren, Y.: A comparison of the physical

837   and optical properties of anthropogenic air pollutants and mineral dust over Northwest China, J.

838   Meteorol. Res., 29, 180-200, doi:10.1007/s13351-015-4092-0, 2015.

839   Wang, Y., Wang, R., Ming, J., Liu, G., Chen, T., Liu, X., Liu, H., Zhen, Y., and Cheng, G.: Effects

840   of dust storm events on weekly clinic visits related to pulmonary tuberculosis disease in Minqin,

841   China, Atmos. Environ., 127, 205-212, 2016.

842   World Meteorological Organization (WMO), Report of the Experts Meeting on Aerosols and Their

843   Climatic Effects, WCP-55, Geneva, Switzerland, 1983.

844   Wu, F., D. Zhang, J. Cao, H. Xu, and Z. An: Soil-derived sulfate in atmospheric dust particles at

845   Taklimakan desert, Geophys. Res. Lett., 39, L24803, doi:10.1029/2012GL054406, 2012.

846   Wu, F., D. Zhang, J. Cao, T. Zhang, and Z. An: Background-like nitrate in desert air, Atmos.

847   Environ., 84, 39-43, 2014.

848   Xia, X., Chen, H., Goloub, P., Zhang, W., Chatenet, B., and Wang, P.: A compilation of aerosol

849   optical properties and calculation of direct radiative forcing over an urban region in northern

850   China, J. Geophys. Res., 112, D12203, doi:10.1029/2006JD008119, 2007.

851   Xu, J., Bergin, M. H., Greenwald, R., Schauer, J. J., Shafer, M. M., Jaffrezo, J. L., and Aymoz, G.:

852   Aerosol chemical, physical, and radiative characteristics near a desert source region of

853   northwest China during ACE-Asia, J. Geophys. Res., 109, D19S03, doi:10.1029/2003JD004239,

854   2004.

855   Yang, M., Howell, S. G., Zhuang, J., and Huebert, B. J.: Attribution of aerosol light absorption to

856   black carbon, brown carbon, and dust in China–interpretations of atmospheric measurements

857   during EAST-AIRE, Atmos. Chem. Phys., 9, 2035-2050, doi:10.5194/acp-9-2035-2009, 2009.

858   Zhang, X., Arimoto, R., and An, Z.: Dust emission from Chinese desert sources linked to

859   variations in atmospheric circulation, J. Geophys. Res., 102, D23, 28041-28047,

860   doi:10.1029/97JD02300, 1997.

861   Zheng, Z., Ren, H., and Huang, J.: Analogue correction of errors based on seasonal climatic

862   predictable components and numerical experiments, Acta Physica Sinica, 58(10), 7359-7367,

863 2009.

864 **Figure captions**

865

866 **Table 1.** Overall average and standard deviation of key optical properties at 550 nm (e.g.,
867 single-scattering albedo, asymmetry factor, real part and imaginary part of complex refractive
868 index) for Asian pure Dust (PDU). Ångström wavelength exponent (α) is in the range of 440-870
869 nm. Minimum and maximum values of the optical properties are in parenthesis for each
870 corresponding column. Measuring period and the total number of PDU ($\alpha < 0.2$) and Transported
871 Anthropogenic Dust (TDU, $0.2 < \alpha < 0.6$) days are in the parenthesis for the first and last column,
872 respectively.

Site (sampled period)	SSA (min, max)	ASY (min, max)	Re (min, max)	Ri ($\times 10^{-3}$)	Ångström (440-870 nm)	PDU/days (TDU)
SACOL (2006-2012)	0.932±0.018 (0.888, 0.971)	0.741±0.012 (0.715, 0.771)	1.534±0.044 (1.438, 1.60)	2.251±0.788 (0.913, 5.51)	0.120±0.049 (0.0, 0.198)	38 (97)
Dalanzadgad (1997-2014)	0.930±0.012 (0.912, 0.949)	0.746±0.010 (0.724, 0.766)	1.512±0.046 (1.447, 1.60)	2.407±0.414 (1.649, 3.19)	0.127±0.079 (-0.06, 0.199)	8 (6)
Beijing (2001-2015)	0.917±0.020 (0.863, 0.963)	0.742±0.012 (0.716, 0.769)	1.557±0.043 (1.401, 1.60)	2.801±0.865 (1.032, 6.20)	0.117±0.067 (-0.048, 0.199)	46 (67)
Yulin (2001-2002)	0.907±0.024 (0.863, 0.952)	0.748±0.010 (0.731, 0.771)	1.559±0.038 (1.476, 1.60)	3.564±1.589 (1.370, 7.92)	0.077±0.068 (-0.024, 0.188)	13 (16)
Dushanbe (2010-2015)	0.941±0.012 (0.916, 0.959)	0.739±0.011 (0.710, 0.765)	1.529±0.041 (1.436, 1.60)	2.011±0.551 (1.022, 3.475)	0.128±0.054 (-0.02, 0.198)	26 (95)
Karachi (2006-2014)	0.945±0.012 (0.916, 0.977)	0.741±0.011 (0.714, 0.767)	1.518±0.030 (1.449, 1.60)	1.938±0.561 (0.758, 3.439)	0.141±0.041 (-0.005, 0.20)	83 (286)
Lahore (2007-2015)	0.930±0.014 (0.901, 0.957)	0.740±0.010 (0.721, 0.765)	1.519±0.038 (1.432, 1.60)	2.253±0.611 (1.207, 3.623)	0.136±0.052 (0.023, 0.198)	26 (248)
IASBS (2010-2013)	0.933±0.017 (0.883, 0.958)	0.725±0.011 (0.704, 0.746)	1.572±0.024 (1.525, 1.60)	2.290±0.845 (1.245, 5.029)	0.098±0.050 (0.021, 0.195)	19 (12)
Kandahar (2008/04-06)	0.925±0.013 (0.903, 0.955)	0.729±0.017 (0.700, 0.768)	1.534±0.035 (1.492, 1.60)	2.855±0.775 (1.445, 4.65)	0.147±0.054 (0.00, 0.199)	10 (4)
Dunhuang (2001/03-05)	0.947±0.015 (0.918, 0.970)	0.745±0.013 (0.723, 0.761)	1.547±0.037 (1.494, 1.60)	1.714±0.697 (1.014, 3.14)	0.039±0.029 (-0.003, 0.091)	6 (0)
Dunhuang_LZU (2012/04-05)	0.958±0.007 (0.951, 0.968)	0.741±0.021 (0.707, 0.771)	1.495±0.042 (1.451, 1.580)	1.589±0.292 (1.092, 1.84)	0.153±0.026 (0.117, 0.184)	5 (4)
Inner_Mongolia (2001/04-05)	0.948±0.012 (0.930, 0.960)	0.751±0.006 (0.743, 0.759)	1.499±0.042 (1.426, 1.54)	1.641±0.457 (1.169, 2.45)	0.069±0.054 (0.011, 0.165)	4 (1)
Minqin (2010/05-06)	0.945±0.002 (0.942, 0.947)	0.756±0.014 (0.740, 0.764)	1.469±0.023 (1.449, 1.494)	2.036±0.220 (1.883, 2.29)	0.119±0.023 (0.103, 0.146)	2 (0)
Overall Mean	**0.935±0.014**	**0.742±0.008**	**1.526±0.029**	**2.258±0.556**	**0.113±0.033**	**PDU**
Overall Mean	**0.921±0.021**	**0.723±0.009**	**1.521±0.025**	**3.643±1.372**	**0.355±0.06**	**TDU**

873

874

877 **Table 2.** Spectral optical properties of Pure Dust (α<0.2) and Transported Anthropogenic Dust

878 (0.2<α<0.6) averaged for 13 sites over East and Central Asia areas.

Asian Dust	Pure Dust (α<0.2)	Transported Anthropogenic Dust (0.2<α<0.6)
ω_0(440/675/870/1020)	0.906/0.962/0.971/0.975 ±0.009	0.897/0.943/0.954/0.959 ±0.019
Re(440/675/870/1020)	1.520/1.533/1.517/1.503 ±0.026	1.509/1.533/1.532/1.525 ±0.027
Ri(440/675/870/1020) $\times 10^{-3}$	3.413/1.574/1.449/1.449 ±0.450	5.064/2.737/2.510/2.486 ±1.300
ASY(440/675/870/1020)	0.758/0.727/0.724/0.726 ±0.008	0.736/0.711/0.710/0.712 ±0.009
r_{Vf} (μm); σ_f	0.159±0.029	0.140±0.011
r_{Vc} (μm); σ_c	2.157±0.112	2.267±0.214
Cvf ($\mu m^3/\mu m^2$)	0.037±0.011; 0.06×τ(1020)-0.001	0.038±0.011; 0.12×τ(1020)-0.014
Cvc($\mu m^3/\mu m^2$)	0.632±0.167; 0.88×τ(1020)-0.07	0.343±0.084; 0.90×τ(1020)-0.06
Cvc/Cvf	17.9 (11~31)	9.1 (5~11)

879 Each variable is accompanied by a standard deviation (e.g.., ±0.01). r_{Vf} and r_{Vc} are the volume

880 median radii of fine-mode and coarse-mode particles in μm; Cvf and Cvc denote the volume

881 concentrations of fine-mode and coarse-mode particles in $\mu m^3/\mu m^2$, respectively. The dynamic

882 dependencies of dust optical properties are exhibited as functions of AOD_{1020}, with correlation

883 coefficients greater than 0.93 for all cases.

884
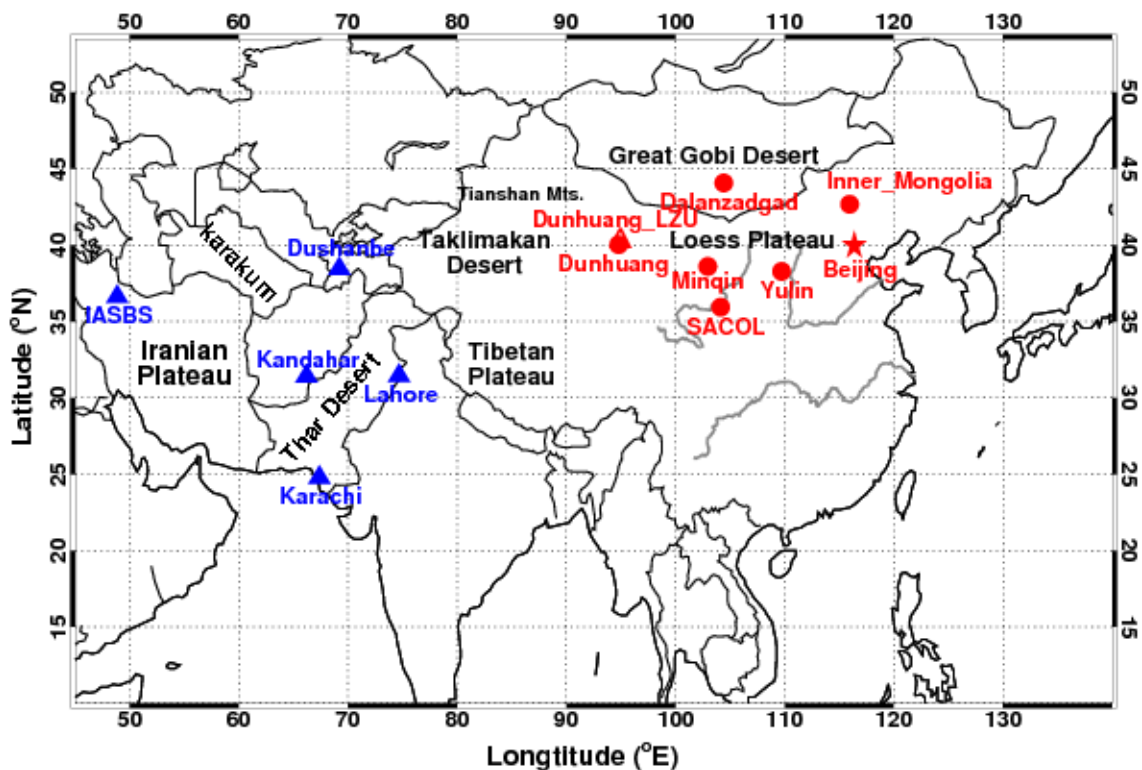
885

886 **Figure 1.** Geographical location of selected 13 AERONET sites in this study. Eight sites over East

887 Asian region are labeled with red colors, and five sites over Central Asian region are labeled with

888 blue colors. The major Great deserts or Gobi deserts along with plateaus are marked with black

889 font.
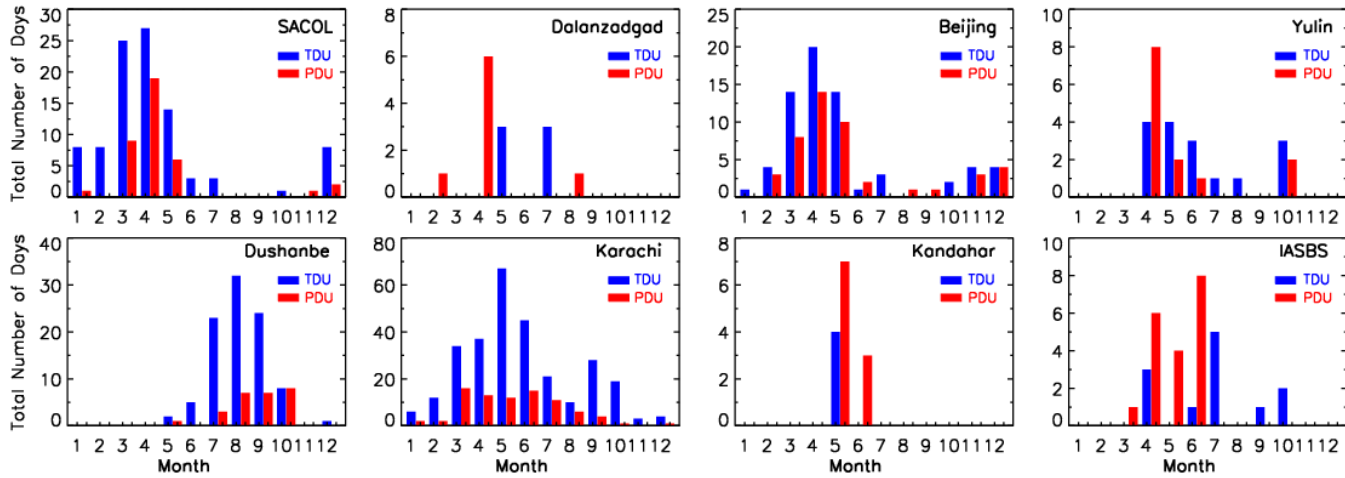
Figure 2. Occurrence frequency of total number days for Pure Dust ($\alpha<0.2$, PDU with red color) and Transported Anthropogenic Dust ($0.2<\alpha<0.6$, TDU with blue color) at selected four East Asian sites (top panel) and four Central Asian sites (bottom panel).
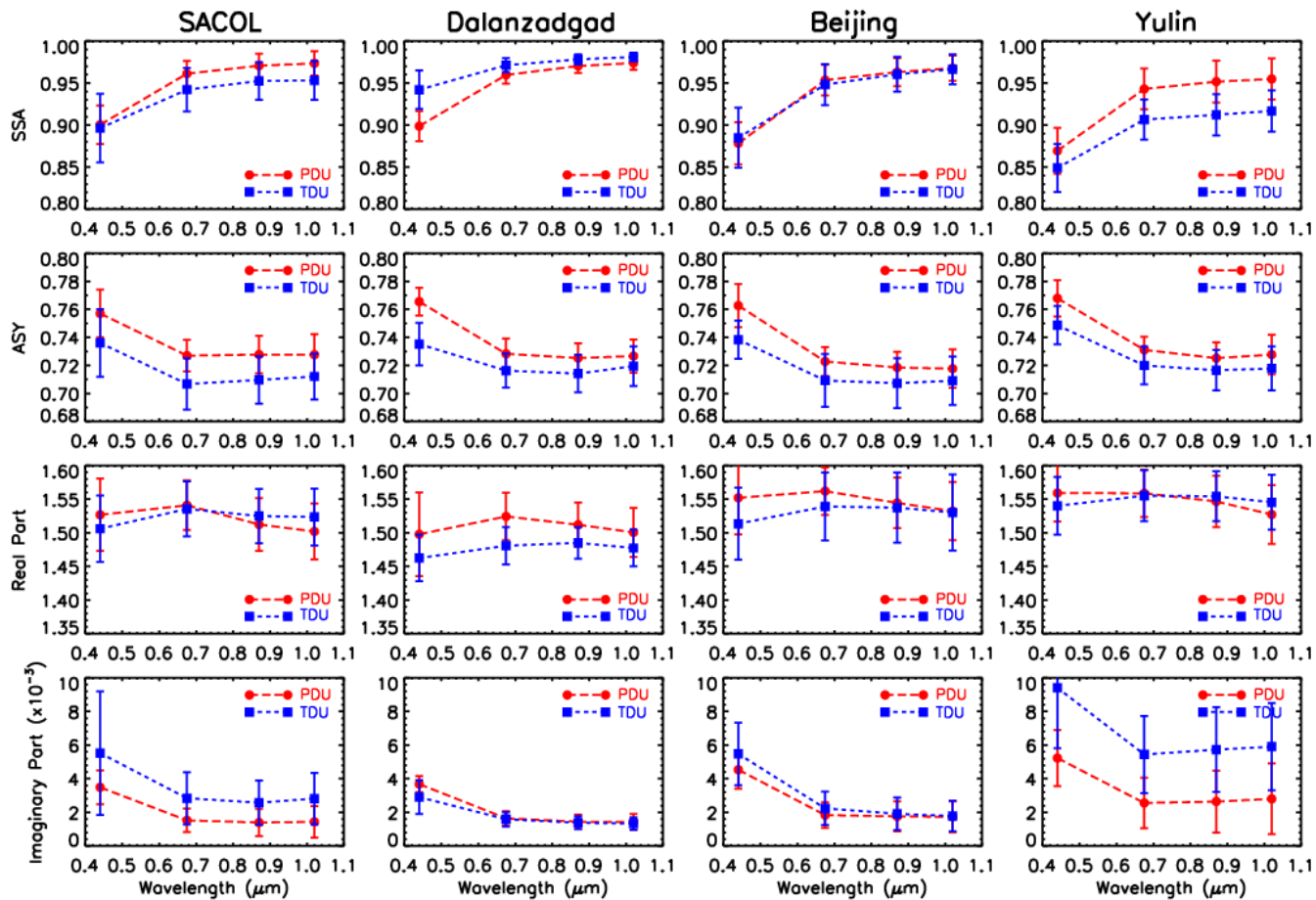
Figure 3. Overall average spectral behavior of key optical properties for Pure Dust ($\alpha<0.2$, PDU with red circle) and Transported Anthropogenic Dust ($0.2<\alpha<0.6$, TDU with blue square) at selected four East Asian sites (SACOL, Dalanzadgad, Beijing and Yulin). The error bars indicate

    plus or minus one standard deviation.
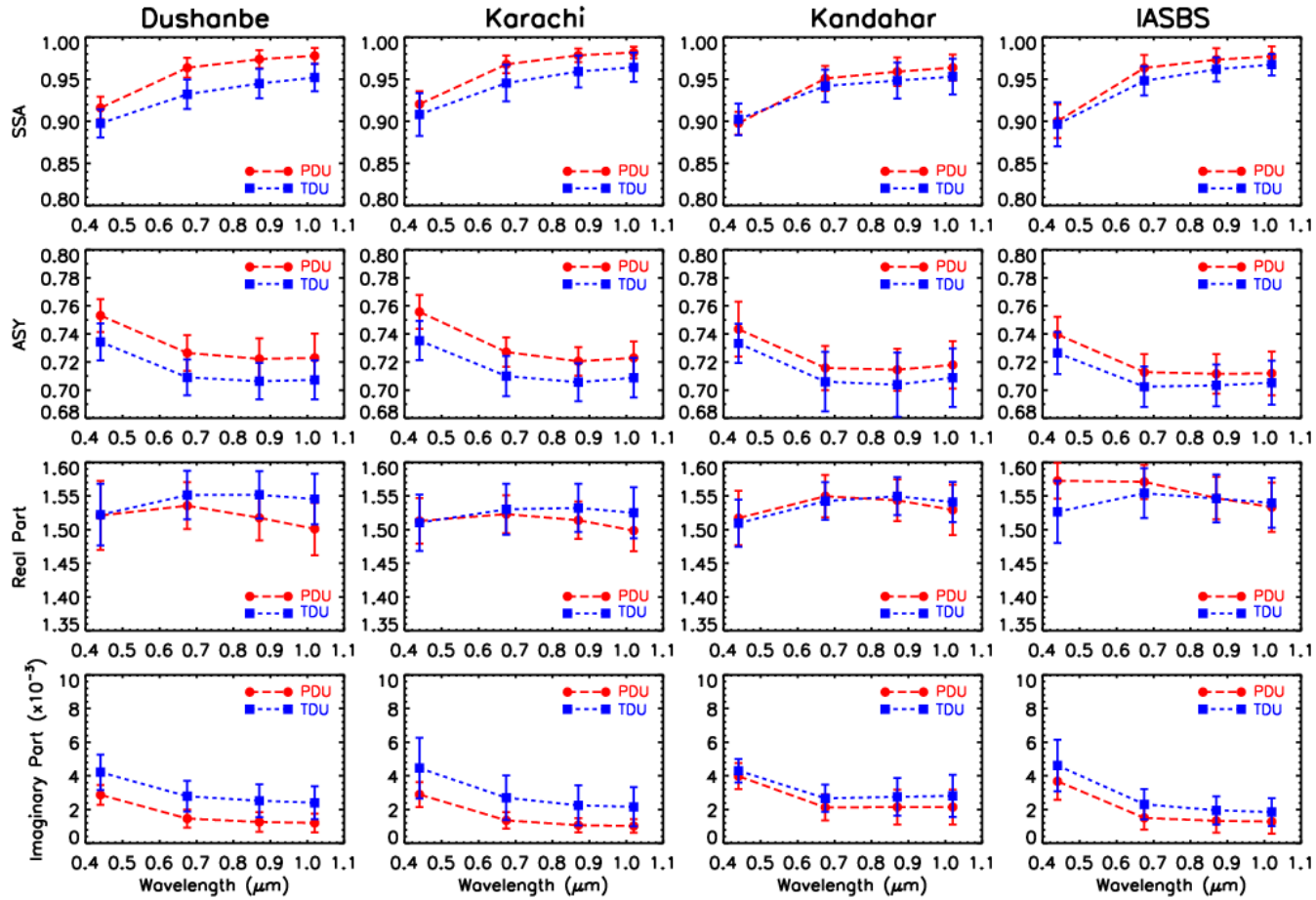
904   **Figure 4.** The same as Figure 3, but for selected four Central Asian sites (Dushanbe, Karachi,

905   Kandahar and IASBS).

906
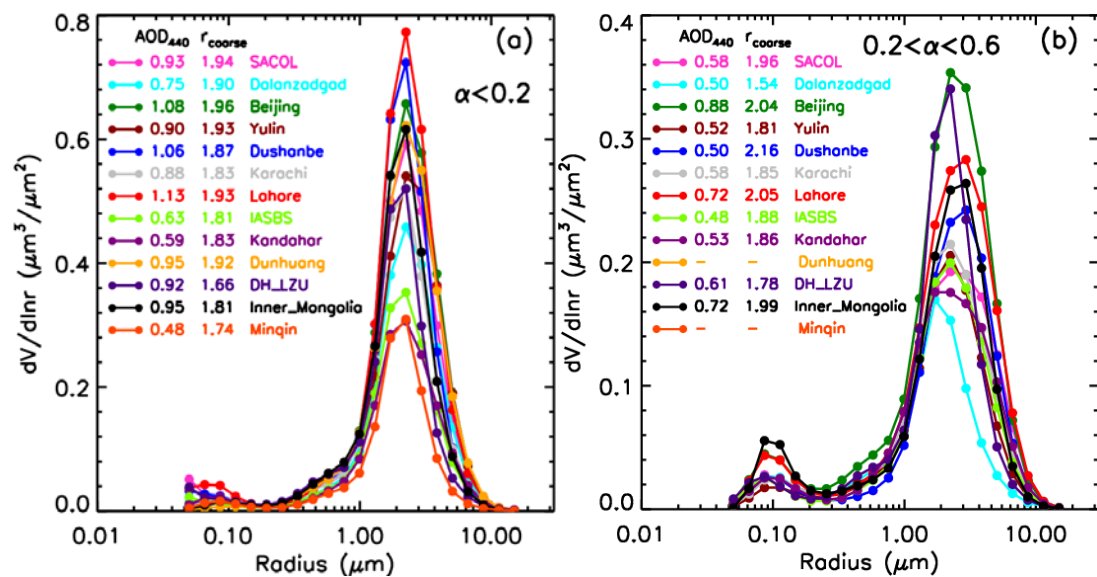
908   **Figure 5.** Overall average of aerosol volume size distributions in the entire atmospheric column

909   for (a) Pure Dust ($\alpha<0.2$) and (b) Transported Anthropogenic Dust ($0.2<\alpha<0.6$) at selected 13

AERONET sites. Corresponding aerosol optical depth at 440 nm (AOD$_{440}$) and effective radius of coarse mode (r$_{coarse}$) in μm are also shown. Note that the "-" in Figure 5(b) represents that missing data for AOD$_{440}$ and r$_{coarse}$ at Dunhuang and Minqin sites.
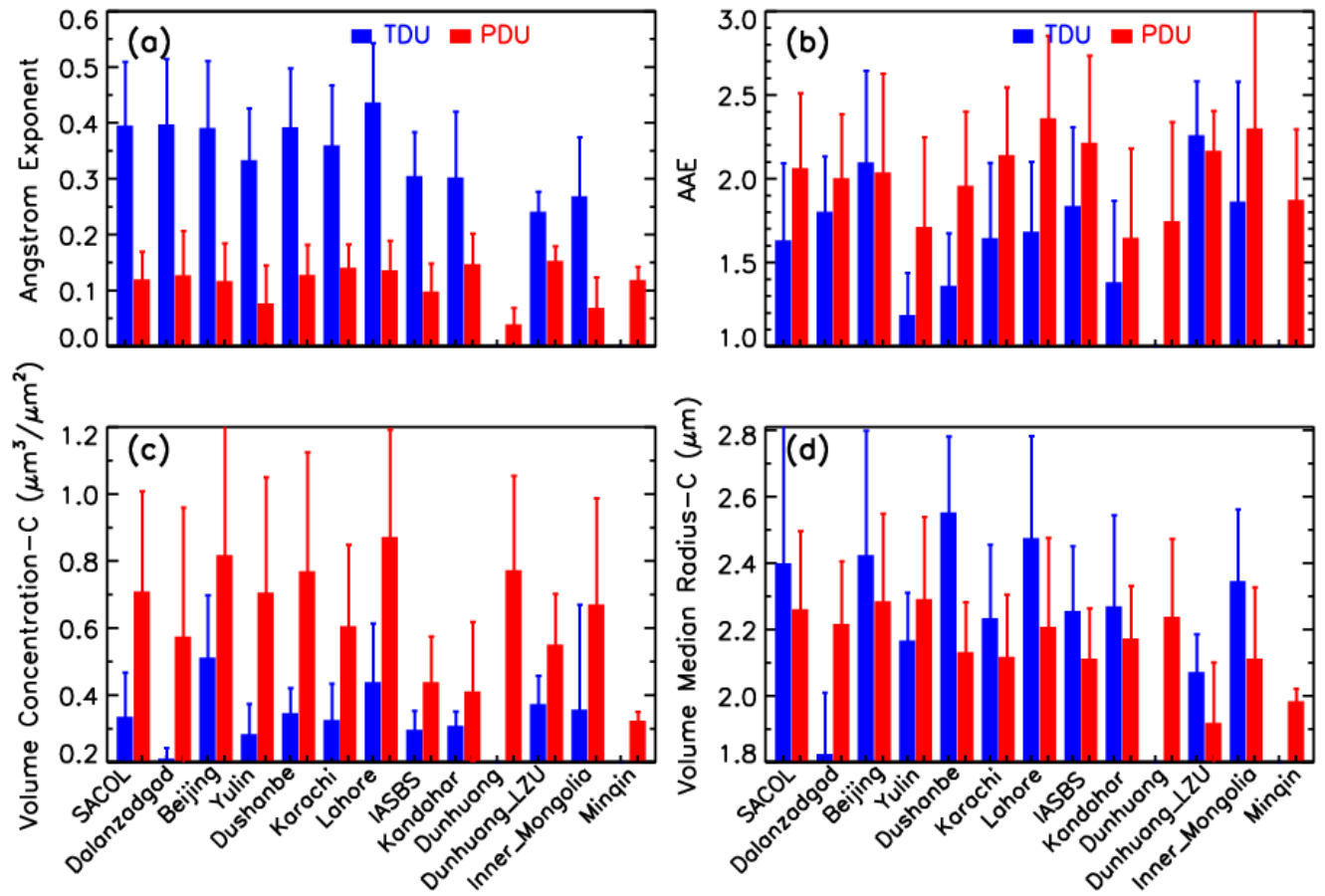
Figure 6. Total average values of (a) Ångström exponent (440-870 nm), (b) absorption Ångström exponent at 440-870 nm (AAE), (c) volume concentration of coarse mode (μm^3/μm^2), and (d) volume median radius of coarse mode in μm for Transported Anthropogenic Dust (0.2<α<0.6, blue color) and Pure Dust (α<0.2, red color) at 13 selected AERONET sites. The error bars indicate plus or minus one standard deviation.

933
934
935
936
937
938
939
940
941

942

943
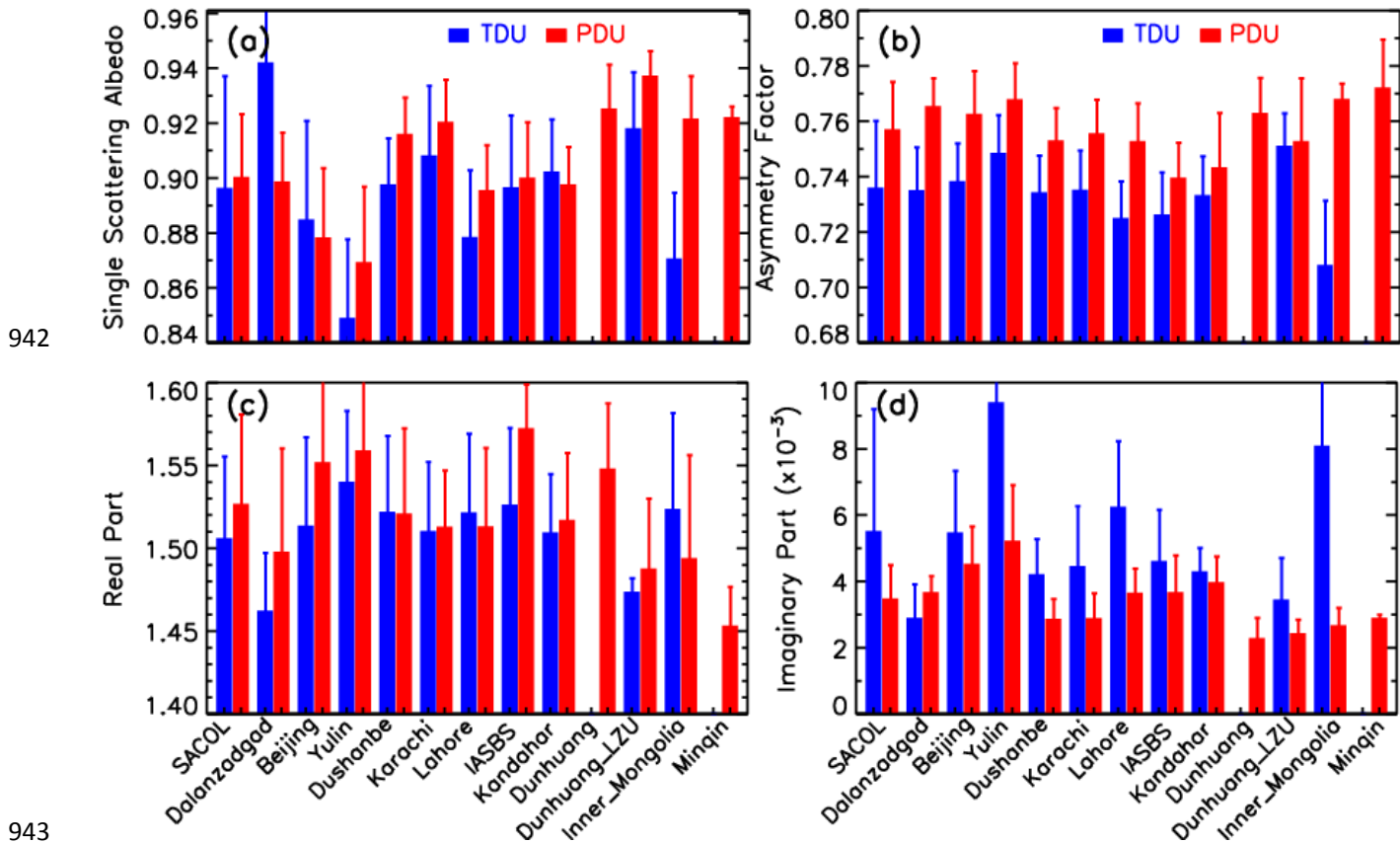
Figure 7. The same as Figure 5, but for (a) sing-scattering albedo, (b) asymmetry factor, (c) real
part and (d) imaginary part of complex refractive index at 440 nm.

946
947
948
949
950
951
952
953
954
955
956
957

958

959

960

961

962

963

964

965

966

967
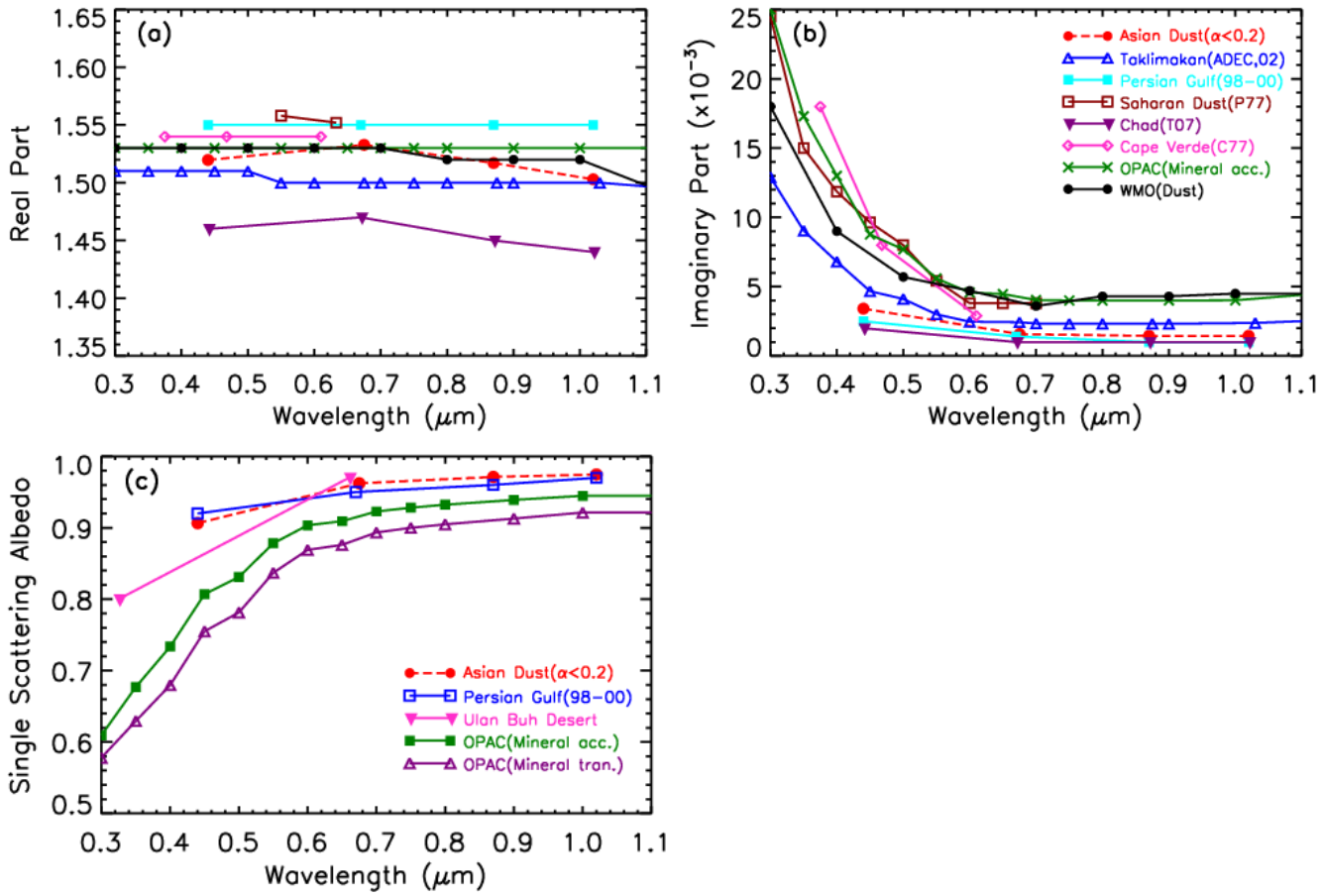
968

969

Figure 8. Mean spectral behaviors of (a) real part, (b) imaginary part of complex refractive index, and (c) single-scattering albedo for Asian Pure Dust (α<0.2) calculated for 13 AERONET sites, and results of current common dust models (OPAC, WMO), Bahrain-Persian Gulf of Desert dust (1998-2000), Saharan dust (Chad, Cape Verde Islands), and Chinese Gobi desert (Taklimakan, Ulan Buh Desert) are also shown for comparison.

975

976

977

978

979

980

981

982

983

984

985

986

987

988

989
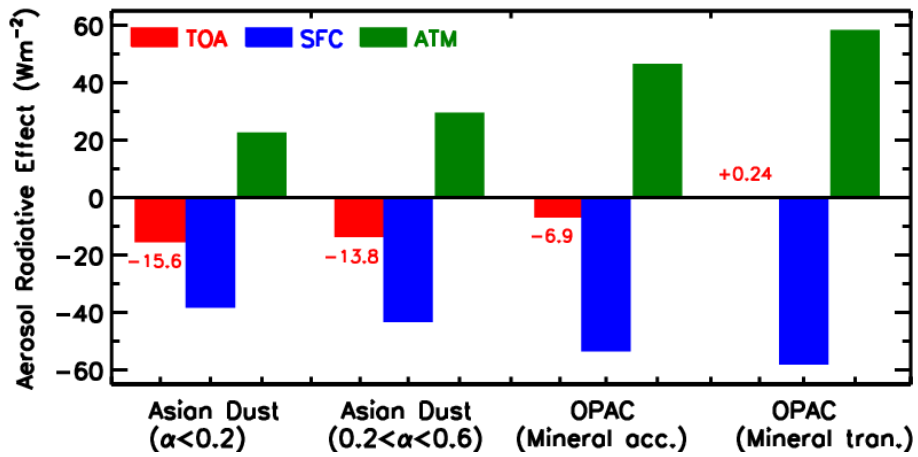
Figure 9. Aerosol shortwave direct radiative effects at the top of the atmosphere (TOA, red color), at the surface (SFC, blue color), and in the atmospheric layer (ATM, green color) for Asian Pure Dust ($\alpha<0.2$) and Transported Anthropogenic Dust ($0.2<\alpha<0.6$) computed in this study, and corresponding values for OPAC Mineral accumulated (Mineral acc.) and transported (Mineral tran.) modes are also presented for comparison.

995